ADDIS ABABA UNIVERSITY

FACULTY OF SCIENCE

Department of Physics

# EXPERIMENTAL STUDIES OF INJECTION ELECTROLUMINESCENCE IN p-n JUNCTIONS



A Thesis

Presented to The

School of Graduate Studies

and

The Faculty of Science

Addis Ababa University

In Partial Fulfillment of the

Requirements for the Degree

of Master of Science in Physics

by

Gelana Amente

June, 1987

ADDIS ABABA UNIVERSITY

School of Graduate Studies

# EXPERIMENTAL STUDIES OF INJECTION ELECTROLUMINESCENCE IN P-N JUNCTIONS

by

Gelana Amente

Faculty of Science

Approved by the Examining Board

Dr. R. Feistel — Feistel
External Examiner

Dr. P. Hruska — [signature]
Advisor

Dr. D. Letov — [signature]
Member

Dr. J. Netchaev — J. Netchaev
Member

C O N T E N T S


| | | Page |
|---|---|---|
| | ACKNOWLEDGEMENT | I |
| | ABSTRACT | II |
| | LIST OF FIGURES | III |
| | LIST OF TABLES | IV |
| | INTRODUCTION | 1 |
| I | THEORY | |
| 1.1 | Injection Mechanisms | 7 |
| | 1.1.1 I-V Relationship in p-n Junction | 10 |
| | 1.1.2 Junction Capacitance | 14 |
| 1.2 | Group III-V Semiconductors | 15 |
| | 1.2.1 Ga (As,P) Ternary Alloys | 16 |
| | 1.2.2 Isoelectronic Centers | 19 |
| 1.3 | Radiative Recombination Processes | |
| | 1.3.1 Possible Radiative Transitions in LEDs | 23 |
| | 1.3.2 Recombination Kinetics in $GaAs_{1-x}P_x$:N | 24 |
| | 1.3.3 Minority Carrier Lifetime | 30 |
| 1.4 | Nonradiative Recombination | |
| | 1.4.1 Defects and Deep Impurity levels | 31 |
| | 1.4.2 Auger Recombination | 32 |
| 1.5 | Degradation in EL Diodes | 33 |

| | | | Page |
|---|---|---|---|
| II | MATERIALS AND METHODS OF MEASUREMENT | | |
| | 2.1 | Sample Specification . . . . . | 35 |
| | 2.2 | Electrical Measurements . . . . . | 36 |
| | 2.3 | Optical Measurements . . . . . | 38 |
| | 2.4 | Thermal Band GaP Measurement . . . . . | 41 |
| III | EXPERIMENTAL RESULTS AND DISCUSSION | | |
| | 3.1 | I-V Characteristics . . . . . | 43 |
| | 3.2 | C-V Characteristics . . . . . | 46 |
| | 3.3 | The Relationship of Photocurrent to Diode Voltage . . . . . | 49 |
| | 3.4 | Electroluminescence Emission Spectra . | 53 |
| | 3.5 | Thermal Band Gap Determination . . | 63 |
| IV | CONCLUSIONS . . . . . | | 66 |
| | REFERENCES . . . . . | | 68 |

ACKNOWLEDGEMENT

I want to pass my cordial thanks to my Advisor Dr. P. Hrushka who has assisted and guided me in this thesis work. I am indebted to all my Lecturers who have shown sinscere cooperation throughout my M.Sc training. I am also grateful to all members of the Physics Department of the AAU who have delivered their unreserved cooperation whole hearted throughout my experimental work.

Last but not least, I would like to thank Ato Girma Dagne who devoted his valuable time and carefully assisted me on the technical part of this thesis.

ABSTRACT

Experimental study of optical and electrical properties of six different groups of electroluminescent diodes (LEDs) was carried out at and near room temperatures. The first category of the diodes consisted of four groups of red (LQ 1131), orange (experimental samples without catalogue number) yellow I (LQ 1431) and green I (LQ 1731) colored LEDs fabricatd by TESLA Electronics, in Czechoslovakia. Each of these groups consisted of seven samples. In the second category, there were two groups of yellow II ($LED_4$ 586-481) and green II ($LED_4$ 586-491) colored LEDs each with three samples. These second category LEDs were fabricated by Radio Spares (RS) of England.

Comparative studies of I-V, C-V. $I_{photo}$ -V, emission spectra and band gap were carried out for all these diodes. The I-V characteristics revealed that the ideality factor 'n' in $I \sim e^{qV/nKT}$ ranges from 1.3 (for orange) to 1.7 (for red) in the first four groups. For yellow II & green II this parameter has values of 1.8 & 1.9, respectively. These values of n remained constant in the exponential region which extended over about two decades of the voltage for most of the diodes.

C-V result indicated that all the diodes have abrupt junctions with built in potentials of 2.89, 1.63, 2.04, 2.14, 1.92 & 2.06 eV for red, orange, yellow I, yellow II, green I & green II, respectively. The $I_{photo}$ vs V study showed that luminosity ($\sim I_{photo}$) has an exponential voltage dependence (of the form $e^{qV/nKT}$) in the voltage range over which the ideality factor (n) nearly remained constant.

Emission intensity peaks were observed for all the LEDs at wavelengths (energies) of 560 nm (2.215eV); 587 nm (2.114eV); 590 nm (2.103eV); 662 nm (1.874eV); 562 nm (2.208eV) and 593 nm (2.092eV) for green I, yellow I, orange, red, green II and yellow II, respectively. Spectral emission study and band gap measurements showed that the LEDs are of Ga (As.P) with the exception of the orange LEDs, which in some cases showed deviations from the values of orange Ga (As.P) LEDs.

Radiative recombinations occured for the red LEDs at an impurity level of about 50 meV and for green at about 40 meV from either band edges. For yellow LEDs the values were as high as 80 meV. An attempt was made to evaluate efficiency of the light emission for the EL diodes. Light emission intensity comparison revealed red LEDs as the most intense followed by green I, the recombination of which might have possibly been assisted by nitrogen isoelectronic traps. The small intensity value in all the rest of the diodes might be attributed to the absence of the isoelectronic traps.

No position shift of the peak emission energy was observed with diode currents for all the EL diodes.

LIST OF FIGURES


| | | Page |
|---|---|---|
| 1. | p-n junction under zero and forward bias | 8 |
| 2. | Compositional dependence of energy gap and schematic energy momentum diagram for Ga $As_{1-x}$ $P_x$ | 17 |
| 3. | Modulus of the wave fn. and probability density of an electron in Ga $As_{1-x}$ $P_x$ : N | 22 |
| 4. | Recombination Model in Ga $As_{1-x}$ $P_x$ : N | 25 |
| 5. | Schematic diagram for I-V measurement | 37 |
| 6. | Schematic of C-V measurement | 38 |
| 7. | Schematic of luminosity measurement and photomultiplier components | 38 |
| 8. | Spectral characteristic measurements | 40 |
| 9. | I-V characteristics | 44 |
| 10. | C-V characteristics | 47 |
| 11. | $I_{photo}$ & $I_{diode}$ vs V | 50 |
| 12. | ln $I_{photo}$ vs ln $I_{diode}$ | 52 |
| 13. | Correction factor for ΦΘY-79 photomultiplier | 54 |
| 14. | Emission spectra (peak magnitude comparison) | 55 |
| 15. | Secondary peak in orange EL diodes | 57 |
| 16. | Secondary peaks in red and green I | 59 |
| 17. | Peak emission position vs diode current | 61 |
| 18. | ln I vs 1/T curve | 64 |

LIST OF TABLES


| | | Page |
|---|---|---|
| 1 | Recombination parameters | 26 |
| 2 | Mean values of ideality factors (n) | 44 |
| 3 | Built-in potentials and subtrate semiconductor material doping concentration | 48 |
| 4 | n' in L ~ exp (qV/n'KT) | 51 |
| 5 | Average peak and binding energies | 62 |
| 6 | Thermal energy gap | 64 |

# INTRODUCTION

Luminescence, is a phenomenon in which light is observed when electrons excited to higher energy states emit photons with energy in the vissible range as they resume lower energy states. In semiconductors, the electrons recombine with holes at the lower energy states. Luminescence is a nonequilibrium condition since the excitation process disturbs the equilibrium. So, thermal emission (where internal equilibrium is maintained) is not classified under luminescence.

Light can be generated in almost any material under the influence of sufficiently high energy. The energy can be supplied in the form of light, by particles moving with high velocities, by electric fields (currents) etc. The type of luminescence is usually characterized by the excitation mechanisms which involve photons as in photoluminescence, fast moving electrons as in cathodoluminescence and electric fields or currents as in electroluminescence (EL).

EL is a mechanism by which electrical energy is converted to light energy wherein the emission of light is at a rate far in excess of the thermal equilibrium rate. In EL, the excitation can be carried out intrinsically by exciting the electrons with high electric fields (referred to as field effect) or by applying currents such as in injection, breakdown or tunneling EL. EL which is exhibited in many bulk or undoped materials under high field conditions is due to field effect. A doped junction on the other hand, offers a very efficient and well understood means of generation of excess electrons and holes at the proper energy levels.[1]

Emission of light by injection of minority carriers in p-n junctions under forward bias is the mechanism of operation of Light Emitting Diodes (LEDs). The term LED is generally used for technical applications. This thesis however, exclusively deals with EL in p-n junctions.

Eversince the first luminescence in junctions was observed in SiC crystals (i.e. crystals which have built in p-n junctions) in 1923[2], many attempts have been made to study the emission of light in junctions. Particularly lately, possible ways of both radiative and nonradiative transitions were studied for different materials as a result of which many recombination kinetics equations have been developed. This has brought about a new level of knowledge in semiconductor junctions.

LEDs are used as display elements, indicators and optocouplers (which have wide use in opto electronics) on account of their small size, relatively small heat dissipation, fast rise time, endurance under mechanical strain, and better suitability because of their potential for their eye catching brightness. Besides, their use as a supplement to the existing light sources (though the condition of large semiconductor lamps is still on the research stage) and their ability to operate under certain specific conditions still increases their importance in some respects. For instance, yellow green GaP LEDs show excellent match with the eye sensitivity better than any of the presently existing light sources[3]. The constancy of efficiency as their size decreases puts LEDs on top for small size illumination. Their broad spectral output is also one of the reasons which escalates their demand as multicolor indicators.

Unlike other light sources, end of life in LEDs is not associated with catastrophic failure but only indicates reduction in intensity; a sign which could be taken as a warning. LEDs are endowed with long service life which exceeds that of incandescent lamps by at least two to three orders of magnitude[4]. According to Chin et al[5] mean time to failure in LEDs is given as $\sim 10^7$ hrs at 60°C & $6\times10^3$ A/cm$^2$.

Current studies and efforts made to improve LEDs put large emphasis in finding mechanisms to optimize its performance by increasing its efficiency and to minimize degradation (i.e. loss in intensity with long service time). Exploitation of the available colors is also one of the important points which is given due regard. This is a broad field to be tackled both in theoretical and experimental physics.

Improvement of LEDs basically focuses on the improvement of radiative recombination mechanisms. It can be done by selection of proper material type and suitable technology.

In order to qualify as an efficient LED material, a semiconductor must have as a first requirement, band gap of energy greater than 1.8eV[6]. Assuming direct transition from the bottom of the conduction band to the top of the valence band, the energy of the emitted photon is given as

$$E_g = h\nu = h\,c/\lambda = \frac{6.625\times10^{-34}\times3\times10^{8}\ \text{J-sec m/sec}}{\lambda}$$

For red light, $\lambda \sim 700$ nm, and $E_g \sim 1.8$eV

As a second requirement, it should produce stable p-n junction without much problem in the production technology and it must provide favorable radiative recombination transitions.

Direct band gapped semiconductors provide more favorable conditions as far as radiative recombination processes are concerned when compared with indirect gap semiconductors. The probability of radiative transition in indirect gapped semiconductors is very small because the momentum conservation law should be fulfilled in these materials as will be explained later.

All of the group IV semiconductors are indirect gap semiconductors and they have smaller energy gaps (with the exception of SiC.) than aforementioned. In SiC however, efficient luminescence is observed even at temperatures greatly exceeding room temperature but the performance of this compound semiconductor is limited by severe technical and economical problems[2,6].

Despite the fact that some of the group III-V compound semiconductors are indirect (and hence inefficient from this view point), they form one of the potential sources of EL materials. The direct band gapped compounds of this group have relatively narrow bandgaps among which the well known is GaAs (Eg = 1.425 eV at 300K)[7] which emits in the infrared region. The remaining direct gapped semiconductors of this group have either crystal growth or electrical conductivity problems. Compounds of this group are more of ionic type when compared with group IV semiconductors. As one moves from the central IV column of the periodic table towards the relatively more ionic bonded compounds, the [illegible]ure, group II-VI semiconductors have larger band gaps than even group III-V compound semiconductors. The relatively larger energy gapped compounds to

the contrary are characterized by poor mobilities and perhaps inability to promote conductivity of both types of carriers (i.e. electrons & holes). In other words, due to this latter problem, junction formation is difficult or impossible in such compounds. The two constraints can be surmounted by selecting compounds of lighter atomic constants from the higher rows of the periodic table.

Most of the binary compound III-V semiconductors that have an advantage of larger energy gap are indirect, but the inefficiency due to the indirect gap can be improved by introduction of proper types of impurities such as isoelectronic traps.

The core in the study of the performance of LEDs lies in finding the causes of radiative and nonradiative recombinations and ways of enhancing the radiative ones. The quantitative dominance of radiative recombinations over nonradiative recombinations indicates light emission. Since indirect band gaps favor nonradiative recombinations, impurites play prominant role in the indirect region and greatly influence the efficiency. The study of the electrical and optical characteristics of LEDs is thus linked with the role of different types of impurities in semiconductors. Studies of such parameters indicate the status of LEDs.

In this work, I-V, C-V & LIV characteristics were studied. Besides emission spectra and thermal band gap measurements were taken for 34 samples of commercial LEDs at and near room temperatures. In the results, some of the quantitative parameters obtained in the study were given in the from of tables. Attempts were also made to correlate some of these parameters

with radiative recombination processes. The discussions include some qualitative remarks relevant to the performance of the different colored LEDs and to the effect of impurities. The work is more of a comparative type and hence, similarities and differences between the two catagories of LEDs are given in each section.

# I THEORY

## 1.1 INJECTION MECHANISMS

Luminescence in LEDs comprises of three major stages[9]. The first is the excitation process (i.e. injection of minority carriers). In the 2nd part charge transport and capture take place and finally the charges recombine radiatively or nonradiatively.

In binary compound LEDs of group III-V, elements of group VI substituting Group V elements in the compound act as shallow donors and group II elements substituting group III elements act as shallow acceptors. For instance, in group III-V compounds, elements such as (S, Se, Te & Sn) act as shallow donors and (Cd, Zn, Mg, Be) act as shallow acceptors. Ge & Si are amphoteric because they can act as donors or as acceptors[10]. The donors and the acceptors are substitutional impurities since electrically active impurities usually occupy substitutional sites[11].

At room temperature shallow donors and acceptors possess localized energy levels of the order of 26 meV from the conduction and valence bands, respectively[12]. Hence, owing to their low binding energy, they are easily ionized at room temperature unlike deep impurity levels (i.e. states whose energy is close to the intrinsic Fermi level). Shallow donors and acceptors therefore, act as activators of luminescence.

Fig.1 illustrates how injection EL takes place in p-n junctions.

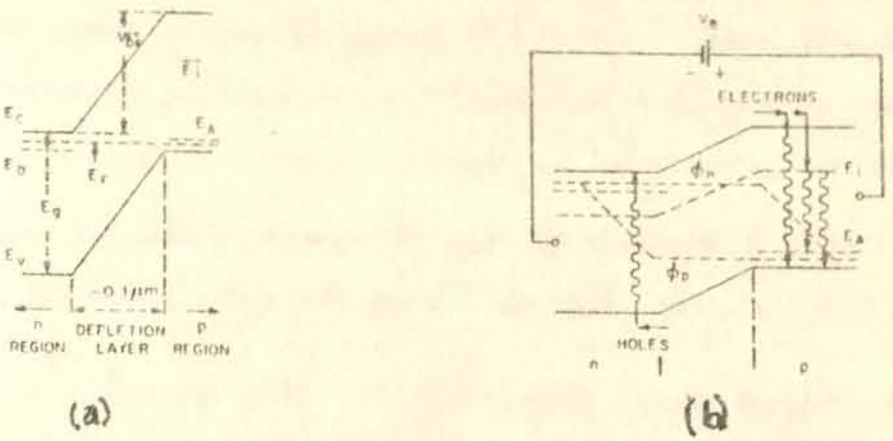


Fig.1(a): Schematic representation of energy states through p-n junction at zero bias. (b): p-n junction under forward bias ($V_F$) conditions. The Fermi level is $E_F$. $\phi n$ & $\phi p$ are quasi Fermi levels, $E_i$ is an impurity state inducing radiation. [After Berah & Dean, 8]

As separate entities, p&n semiconductors have different Fermi energy levels which are dependent on the doping concentrations. In p-n junctions, before equilibrium conditions are reached, electrons and holes flow into opposite sides until an internal electric field is established across the interfacial region. The flow continues until the magnitude of the field is sufficient to stop further flow of charges and the Fermi level on both sides equalized. Electric field arises because of the space charge distributions of the thermally ionized donors and acceptors. The region where the field is builtin is free of mobile charges. Only ionized donors and acceptros are present. This region is referred to as the DEPLETION LAYER.

The location of the Fermi level depends on the doping concentration. For low doping concentration, the diode would be nondegenerate and the Fermi level lies within the forbidden gap below the bottom of the

conduction band ($E_c$) or above the top of the valence band ($E_v$). At higher doping concentrations, $E_F$ lies within the conduction or valence band depending upon the high doping concentration of donors or acceptors. In most LEDs, one side is always degenerate[13] because of the following two reasons.

i) The barrier height reduces by the value of $\xi$, where $\xi$ is the energy difference between Ec and the new Fermi level.

ii) In the heavily doped side band filling rises the threshold energy absorption by $\xi$ such that the emitted light traverses this smaller side without much absorption.

At zero bias, there is no net current since the number of minority carriers which are being swept down the potential barrier is compensated by the same number of few majority carriers which can overcome the potential barrier.

At forward bias, the energy barrier decreases in proportion with the magnitude of the applied voltage. The number of the minority carriers which are swept down the potential barrier remain constant but the number of majority carriers overcoming the newly reduced potential barrier increases. These majority carriers become minority as they cross the junction and hence, the name minority carrier injection.

The injected minority carriers may recombine within the depletion region or within a diffusion length distance from the depletion region. Most of the recombinations within the depletion region are nonradiative while recombinations outside the depletion region may be radiative or nonradiative depending on the location of the impurity levels[14,15].

Under forward bias, two quasi Fermi levels appear corresponding to each carrier within the depletion region. These two levels describe the concentration of injected minority carriers although these carriers are not in thermal equilibrium with the majority carriers[16]. The separation of the quasi Fermi levels implies that a shallow donor-acceptor may be filled with electrons or holes only near the n or p sides of the junction but both will be ionized elsewhere within the junction. Deep levels which act as recombination centers may lie within the quasi Fermi levels throughout the junction whereas the recombination at shallow levels can be significant only near the edges of the depletion region or within the minority carrier diffusion length in the n and p region adjacent to the junction[17].

1.1.1 Current Voltage Relationship in p-n Junctions

In ideal diodes, no recombination is assumbed to occur within the depletion region and the only current in such diodes is diffusion current, which is caused by the diffusion of majority carriers into the minority side on account of the reduced barrier height. Using the continuity and Poisson equations and assuming small injection, the ideal diode equation is given by [18]

$$I = (I_{no} + I_{po})[\exp(qV/KT) - 1] \qquad (1)$$

where $$I_{no} + I_{po} = q\, \bar{n}_i^2\, [(D_n/L_n)N_A + (D_p/L_p)N_D]$$

$D_p$ & $D_n$ are diffusion coefficients and $L_p$ & $L_n$ are diffusion lengths of holes and electrons respectively. $N_A$ & $N_D$ are concentrations of acceptors and donors & $n_i$ is the intrinsic carriers concentration,

Eqn.(1) only holds in narrow band gapped semiconductors. In dioden with larger energy gaps, several additional factors contribute to the diffusion current as a result of which modification of eqn.(1) is required.

Underforward bias, eqn.(1) is affected by [19]

i) recombination of carriers in the depletion region,

ii) series resistance effect which results in voltage drop acorss the bulk and contacts of the semiconductor and has significant effect at large forward bias,

iii) high injection current wherein at relatively large forward bias the minority carrier density becomes comparable to the majority carrier density,

iv) tunneling current effect at low forward bias and

v) surface effects caused by defects on the surface that link the conduction band states to the valence band states and create a shunt path.

At an intermediate bias (i.e. voltage range over which most LEDs show relatively efficient performance), only recombination current competes with diffusion current and the influence of the effect of all the others can be neglected. According to Sze[20] recombination rate R (in units of $cm^{-3}/sec$) is given by

$$R = \frac{\sigma_p \sigma_n V_{th}(pn - ni^2) N_t}{\sigma_n \left\{n n_1 \exp[(E_t-E_i)/KT]\right\} + \sigma_p \left\{p+n_1 \exp[(E_t-E_i)/KT]\right\}} \qquad (2a)$$

where $\sigma_p, \sigma_n$ are the hole and electron capture cross-sections, respectively, $V_{th}$ the carrier thermal velocity, $N_t$ the trap density, $E_t$ the trap energy level, $E_i$ the intrinsic Fermi level and $n_i$ the intrinsic carrier density.

At nonequilibrium conditions,

$$pn = n_i^2 \exp(qV/KT)$$

Hence, substituting for pn in eqn. (2a) yields

$$R = \frac{\sigma_p \sigma_n V_{th} N_t n_i^2 [\exp(qV/KT) - 1]}{\sigma_n \{n + n_i \exp[(E_t - E_i)/KT]\} + \sigma_p \{p + n_i \exp[(E_i - E_t)/KT]\}} \quad (2b)$$

Using the assumptions that $E_i = E_t$ and $\sigma_n = \sigma_p = \sigma$,

$$R = \frac{\sigma V_{th} N_t n_i^2 [\exp(qV/KT) - 1]}{n + p + 2n_i} \quad (2c)$$

But, since $n = n_i \exp[q(\Psi - \phi_n)/KT]$ and

$p = n_i \exp[q(\phi_p - \Psi)/KT]$

Where $\Psi$ is the potential of the intrinsic level, R assumes maximum value in the depletion region when $\Psi = (\phi_n + \phi_p)/2$

$$R = \frac{\sigma V_{th} N_t n_i^2 [\exp(qV/KT) - 1]}{n_i \{\exp[qV/2KT] + \exp[qV/2KT] + 2\}} \quad (2d)$$

For $V > kT/q$ eqn.(2d) reduces to

$$R = (1/2)\sigma V_{th} N_t n_i \exp(qV/2KT) \quad (2e)$$

The recombination current density is given by

$$J_{rec} = \int_0^W qR\,dx \simeq (qw/2)\,\sigma\, v_{th} N_t n_i \exp(qV/2KT) \qquad (3a)$$

where W is the depletion layer width.

Therefore, the total forward current density for $p_{no} >> n_{po}$ and $V > (2KT)/q$ is given as

$$J_F = q(Dp/\tau_p)^{1/2} (n_i^2/N_D) \exp(qV/KT) + (qw/2)\,\sigma\, v_{th} N_t n_i \exp(qV/2KT) \qquad (3b)$$

This, for junction of constant area reduces to

$$I = I_s \exp(qV/KT) + I_r \exp(qV/2KT) \qquad (4)$$

The first term on the right gives the diffusion current and the second with a factor of half in the exponential term represents the recombination current. $I_s$ and $I_r$ give reverse saturation currents of both components. If $(V_{appl} - IR)$ is taken for V in eqn.(14), the IR term takes care of the series resistance effect.

Owing to the fact that the total current depends on two currents which have two different exponential dependence, under forward bias, eqn.(14) could be given in a more compact and experimentally suitable form as

$$I = I_o \exp(qV/nKT) \qquad (5a)$$

where 'n' the ideality factor, is equal to unity for complete dominance of diffusion current over the recombination current and is equal to two for the reverse case. $I_o$ in eqn.(5a) is a complicated parameter which depends on temperature, intrinsic carrier density,

capture cross sections of electrons and holes at the recombination centers, the position of the trap level relative to the intrinsic Fermi level and the concentration of the trapping levels[19].

The reciprocal of the slope of lnI against voltage yields the value of the ideality factor:

$$n = q/K\,T)\ [\partial V/\partial (\ln I)] \qquad (5b)$$

1.1.2 Junction Capacitance

Important information about the nature of the doping concentration and profile at a p-n junction can be extracted from the measurements of the junction capacitance particularly under reverse bias. In this case, the capacitance is mainly affected by doping concentration of donors and acceptors and the capacitance is referred to as depletion layer capacitance. Under forward bias however, rearrangements of minority carrier density brings about diffusion capacitance which contributes to the depletion layer capacitance.

To obtain depletion layer capacitance, starting from Poissons equation and making an abrupt approximation[21]

$$(-\partial^2 V/\partial X^2) = \partial \mathcal{E}/\partial X = \rho(x)/\varepsilon_s$$

$$= (q/\varepsilon_s)[\ p(x)-n(x)+N_D^+(x)-N_A^-(x)\ ] \qquad (6a)$$

$$(-\partial^2 V/\partial X^2) = (q/\varepsilon_s)(N_D-n) \qquad \text{for } 0<x\leq x_n \qquad (6b)$$

$$(-\partial^2 V/\partial X^2) = -(q/\varepsilon_s)(N_A-p) \qquad \text{for } -x_p\leq x<0. \qquad (6c)$$

Integrating these equations twice yields,

$$V(x) = \mathcal{E}_m[x - (x^2/2w)] \quad \text{where } |\mathcal{E}_m| = q(N_D-n)x_n \quad \mathcal{E}_s = (N_A-p)x_p \quad \mathcal{E}_s \tag{7}$$

$$V_{bi} = (1/2)\,\mathcal{E}_m W = (1/2)\,\mathcal{E}_m\,(x_n+x_p) \tag{8}$$

$$W = \left\{(2\,\mathcal{E}_s/q)[(N_A+N_D)/N_AN_D](V_{bi}-2KT/q)\right\}^{1/2} \tag{9a}$$

which for one sided abrupt junction gives

$$W = [(2\,\mathcal{E}_s/q)N_B)(V_{bi} - 2KT/q)]^{1/2} \tag{9b}$$

where $N_B = N_D$ or $N_A$ .

Evaluation of the depletion layer capacitance using this given value of depletion layer width results in

$$C = (dQc/dV) = d(qN_BW)/d[(qN_B/2\,\mathcal{E}_s)W^2]$$

$$= \mathcal{E}_s/W = [(q\,\mathcal{E}_sN_B)/2]^{1/2}[V_{bi}\pm V - 2KT/q]^{-1/2} \tag{10a}$$

The '+' sign is for reverse bias and the '-' sign is for forward bias.
From eqn.(10a) the slope of $(1/C^2)$ versus V curve is given by

$$d(1/C^2)/dV = 2/(q\,\mathcal{E}_sN_B). \tag{10b}$$

$N_B$ could be obtained from the slope provided $\mathcal{E}_s$ (i.e. the permitivity) is known. The intercept of the curve (at $1/C^2 = 0$) gives the built in potential.

## 1.2 GROUP III-V SEMICONDUCTORS

Luminescence is observed in many of the binary compound semiconductors of group III-V which consist of both direct and indirect band gap and in group II-VI all of which are direct gapped semiconductors. Nevertheless, only few of these binary compounds have gained commercial interest because

of technological and economic factors. The need for wide band gap semiconductors to obtain wide spectral range has necessitated the use of ternary alloys (i.e. combination of two binary compounds) as practical LEDs since in such alloys energy gap can be altered, at will, by varying the composition.

From among the ternary alloys, $Ga_xAl_{1-x}As$ is important for its direct energy gap which extends upto 1.9eV at 300K and because of the small mismatch between Ga As & Al As compounds[22-24]. $In_{1-x}Ga_xP$ has also a direct transition EL peak which persists upto an energy of $\sim$ 2.2eV ($x_c \simeq 0.74$)[25,26]. Despite the advantages that these two alloys have, $GaAs_{1-x}P_x$ LEDs are leading commercially due to the availability of GaAs substrate and for their ease of growth and junction formation[27].

### 1.2.1 Ga(As,P) Ternary Alloys

The advantage of $GaAs_{1-x}P_x$ ternary alloy over its binary compounds (GaAs & GaP) is its simplicity of growth. Besides, as the compositions of As & P vary in the alloy, the band gap changes from the minimum value in GaAs ($E_g$ = 1.424eV at x = 0) to a maximum value in GaP ($E_g$ = 2.261eV at x = 1)[28]. This shows, that Ga P is added to GaAs for the sole purpose of increasing the energy gap. Ga As is direct energy gapped while GaP is indirect but there exists a critical composition value at which a cross over from direct to indirect takes place (Fig.2). The critical cross over value is $x_c$ = 0.45 at 300K according to Sze[28], Dean[29] and others[30,31] but further investigations by a number of researchers[32-35] have shown that $x_c$ = 0.49 at 300K. Above this critical value, transition from direct

$\Gamma$ (000) to indirect X(100) takes place and most of the electrons reside on the X valley minima. At the cross over point, $E_\Gamma = E_X$ and the corresponding energy (for $x_c = 0.45$) is $E_g = 1.997$ eV (Fig.2a). The minimum energy gap at any arbitrary composition (x) is given for ($x_c = 0.49$) by[36]

$$E_\Gamma(x) = 1.441 + 1.091x + 0.210x^2 \qquad (11a)$$

$$E_X(x) = 1.907 + 0.144x + 0.211x^2 \qquad (11b)$$

In LEDs, the color is determined mainly by the energy gap and hence the composition variation alters the color. For instance, in GaAs(As,P) LEDs, $GaAs_{0.6}P_{0.4}$ emits red ($\lambda = 649$nm), $GaAs_{0.35}P_{0.65}$ emits orange ($\lambda = 632$nm) $GaAs_{0.15}P_{0.85}$ emits yellow ($\lambda = 589$nm) and GaP emits green ($\lambda = 570$nm)[37].

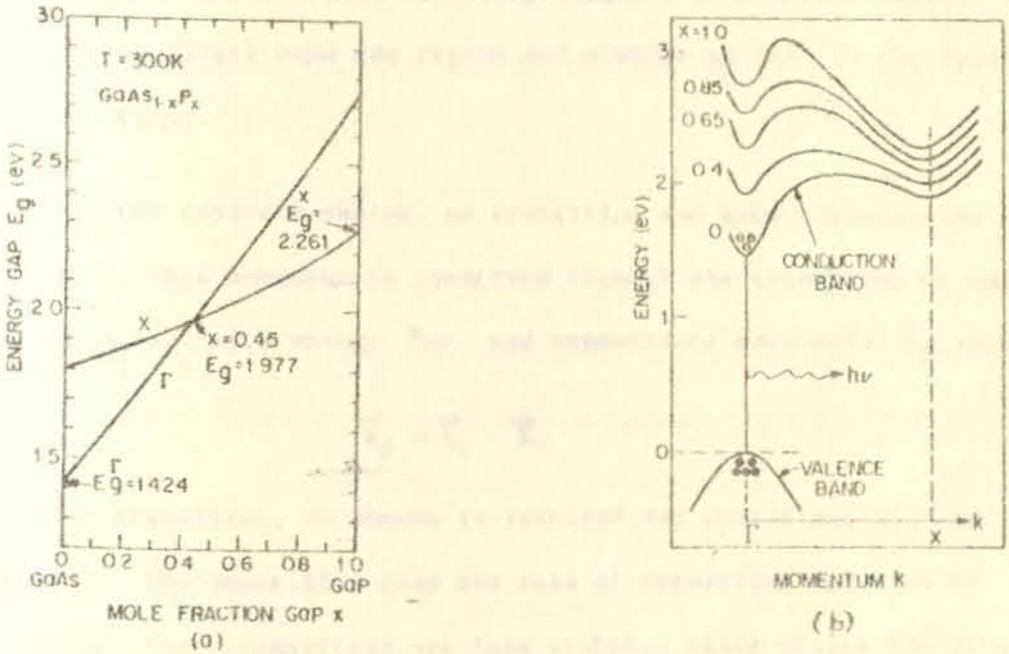


Fig.2: (a) compositional dependence of the direct and indirect energy bandgap for $GaAs_{1-x}P_x$. (b) Schematic energy and momentum diagram for $GaAs_{1-x}P_x$ for different alloy compositions [After Sze[28]]

As seen in Fig.2., when x is increased, the [000] or $\Gamma$ conduction band minima shift upward and there is a direct-indirect transition as [100] or X minima become lowest in energy. This takes place for $x > 0.45$.

The series resistance and the forward bias voltage of the diodes increase with the phosphorous content of the crystal. The increasing composition of As in the alloy besides reducing the indirect band gap enhances the absorption coefficient at or very near the band gap due to free excitons and free hole electron pairs[22]. The reason for the enhancement of this absorption is due to the fact that momentum is conserved by scattering at the As impurities.

Lightly doped diodes of Ga(As,P) behave in a manner similar to GaAs in the direct band gap region and similar to GaP in the indirect band gap region.

In the indirect region, no transition can take place without impurity assistance. Here momentum is conserved through the absorption or emission of phonons each with energy $\hbar\omega$ and appropriate wavevector $\vec{K}_p$ such that:

$$\vec{K}_p = \vec{K}_c - \vec{K}_v \qquad (12)$$

In direct transition, no phonon is involved and photon momentum is negligible. The impurities play the role of conserving momentum by scattering. Such transitions are less probable since unlike the direct transitions, in the indirect transitions the availability of phonons with suitable momenta is essential.

Low radiative recombination probability for intrinsic luminescence is because of second order nature of interband transition in indirect gap semiconductors. The need for impurity centers such as isoelectronic traps which significantly increase the radiative recombination in indirect band gapped semiconductors is therefore very high.

1.2.2 Isoelectronic Centers

The efficiency loss in the indirect region of $GaAs_{1-x}P_x$ alloys is improved by an introduction of isoelectronic traps to the crystal. An isoelectronic trap is an atom of the same valence as the host atom but with larger electronegativity if it is lighter (i.e. in the upper row of the periodic table) than the host atom[38]. This is because of the relatively exposed nuclear charge and it acts as an electron trap. Alternatively, if the substituent atom is heavier, it acts as a hole trap. Once the electron is bound, the isocenter is charged and a hole is readily trapped in the resulting long range potential to form a bound exciton.

An exciton is a mobile combination of an electron and a hole at a certain distance from each other. Exciton states are formed through Coulomb interaction between free electrons and holes. If the excitons are bound to ionized impurities, they are referred to as bound excitons. Such bound excitons can decay (i.e. the electrons and holes can recombine) at the impurity states or at the isotraps.

An isoelectronic center is obtained by doping the ternary alloys with atomic N or $B_i$, or molecules like Zn-O or Cd-O [10]. They are referred to as atomic or molecular isoelectrons, respectively. The

elemental isoelectrons substitute one of the host atoms whereas the molecular isoelectrons substitute either of the two host atoms. In the case of Ga(As,P), doping with nitrogen results in replacement of nitrogen for phosphorous to produce an electron trap level. The binding energy of N is about 10 meV but it has a large capture cross section[22,39]. Hence, N is a shallow isoelectronic trap in $GaAs_{1-x}P_x$ : N unlike $Zn_{Ga}$-$O_P$ in Ga P that induces a relatively deep recombination level as a result of which a low energy red EL is observed.

The mechanism by which an isoelectronic trap enhances radiative recombination is described from the view point of the nature of the electron wave function in the presence of nitrogen in $GaAs_{1-x}P_x$.

The modulus of the wave function of an electron bound to a nitrogen isoelectronic trap in $GaAs_{1-x}P_x$ : N is enhanced near $\vec{K} = 0$ because of the presence of $\Gamma$ conduction band minima. When an electron is bound to the immediate vicinity of the nitrogen impurity, it is acted upon by a short range potential. As the trapped electron binds a hole and an exciton is formed, the exciton is bound to the immediate vicinity of the N impurity. The hole is acted upon by a long range Coulomb potential. In this case, the wave function of the electron and the hole overlap. Due to the overlap, no phonon is involved during the radiative transitions (even if the transition is indirect) when the bound excitons decay[34]. In other words, isotraps change the indirect energy gap to a quasi direct one. They have adverse effects in the direct band gap region.

The mechanism by which the nitrogen isoelectronic trap enhances the radiative recombination in the indirect region is referred to as the Band Structure enhancement (BSE).

In an isoelectronic trap, the potential associated with N isoelectronic impurity is of a short range nature. Campbell et al[34] gave a qualitative description of the behavior of N in ternary $GaAs_{1-x}P_x$ : N starting with the one electron Schrödinger equation and obtained the modulus of the wave function of the bound electron in momentum representation in the form of

$$\left|\Phi_c(\vec{K})\right|^2 = B\left\{\sum_\alpha C_\alpha \left[\beta_\alpha/(\beta_\alpha^2-1)^{1/2}-1\right]\right\}^{-1} (E_c - E_N)^{-2} \qquad (13)$$

where B is a constant and $\beta_\alpha = (E_\alpha + \Delta_\alpha - E_N)/\Delta_\alpha$. $E_\alpha$ is the conduction band edge in the region of the Brillouin zone labeled $\alpha$, $\Delta_\alpha$ is a measure of the extent in energy of the conduction band in the $\alpha^{th}$ region and $C_\alpha$ is the normalization constant.

The probability density $\left|\Phi_c(\vec{K})\right|^2$ is strongly affected by the value of $(E_C - E_N)$ in the denominator of eqn.(13) $E_C = E_\Gamma$ at the $\Gamma$ conduction band edge. As shown in Fig.3, $E_\Gamma$ & $E_N$ come closer in the region a little bit greater than the cross over point. This shows BSE in this region.

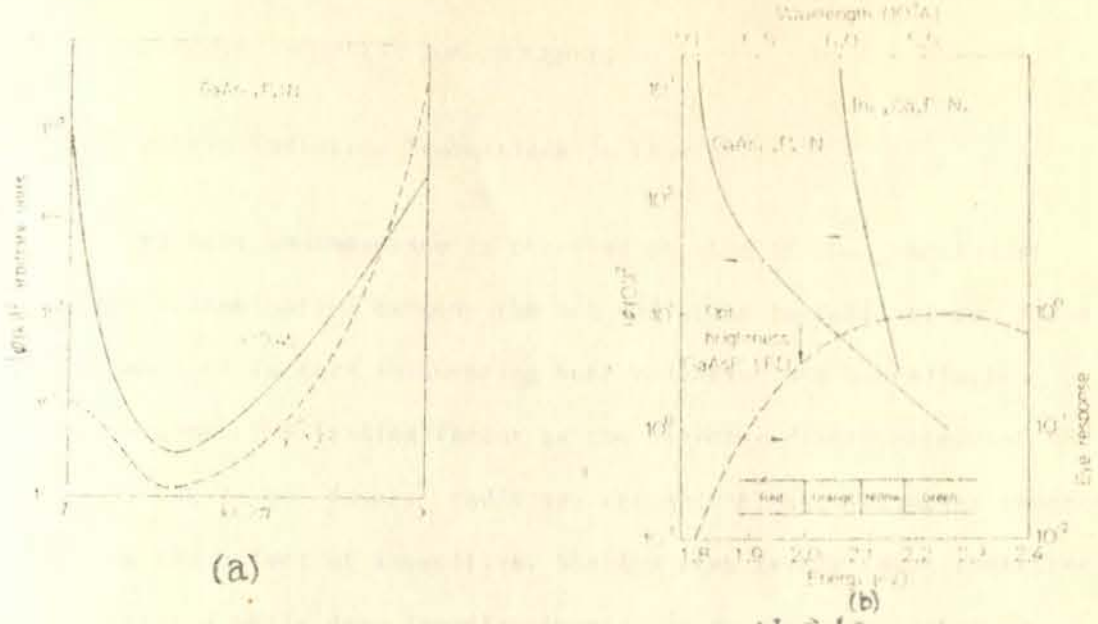

(a) (b)

Fig.3: (a) Modulus of the wave function $|\Phi(\vec{K})|^2$, of an electron bound to N isoelectronic trap in Ga $As_{1-x}$ $P_x$:N along the symmetry line of the Brillouin zone. (b) Probability density, $|\Phi_c(0)|^2$ of the bound electron at $\vec{K} = 0$ ($\Gamma$) in Ga $As_{1-x}$ $P_x$:N. The optimum brightness lies near the red orange boundary, but the variation is relatively small throughout the red yellow spectral range. [After Campbell[34]]

$|\Phi_c(\vec{K})|^2$ has a local maxima at $\Gamma$ which is due to the BSE. The effect of BSE on no-phonon radiative transition is accentuated by order of magnitude as $E_\Gamma$ approaches $E_N$. For Ga $As_{1-x}$ $P_x$ : N , as x decreases from x = 1 near $\vec{K} = 0$ the magnitude of $|\psi_c(\vec{K})|^2$ increases until at $x_c = 0.45$ the probability density at $\Gamma$ exceeds the value at X.

$|\Phi_c(0)|^2$ determines the probability density for radiative bound exciton recombination. Hence, an increase in $|\Phi_c(0)|^2$ indicates an increase in the radiative recombination.

The isoelectronic trap has its optimum effect near the transition region as compared to the region where $x \sim 1$. Thus, the optimum range to fabricate Ga $As_{1-x}$ $P_x$ : N LEDs is $0.6 < x < 0.8$[34].

## 1.3 RADIATIVE RECOMBINATION PROCESSES

### 1.3.1 Possible Radiative Transitions in LEDs

Efficient luminescence is observed in LEDs if the fraction of radiative recombination exceeds the non radiative recombinations. There are a number of factors influencing both radiative and nonradiative recombinations. The leading factor is the direct-indirect nature of the band gap. The former favors radiative recombinations. The other important factor is the effect of impurities. Shallow trap levels favor radiative recombinations while deep impurity levels, vacancies, precipitates, dislocations etc., enhance nonradiative processes. Yet, in some cases (say in indirect gap semiconductors), a relatively deep donor and acceptor levels are preferred to very shallow levels for efficient radiative recombinations[13]. This is because

i) with deep impurities momentum conservation is easier due to the extension of the wave function throughout the momentum space.

ii) recombination at nearest pairs does not require tunneling.

Transitions in LEDs can take place in one of the following ways:

i) band to band (intrinsic).

ii) free to bound or viceversa on donors, acceptors or isotraps

iii) pair recombination at shallow donors and acceptors, and

iv) bound exciton recombination at shallow impurities such as iso-substituents.

In indirect transition, selection rule demands momentum conservation by ionized impurity scattering.

In nitrogen doped materials, decay of excitons to bound nitrogen atoms dominate and in nitrogen free materials exciton recombination previals. The free to bound transitions are on the donors or acceptors in the absence of nitrogen[39].

1.1.2 Recombination Kinetics in Ga $As_{1-x}$ $P_x$ : N

According to Campbell et al[34], Ga P : Zn-O, Ga P : N & Ga $As_{1-x}$ $P_x$:N have nearly the same recombination models (as shown in Fig.4) since all of them incorporate isoelectronic traps. The three states of a nitrogen isoelectronic impurity are

i) the impurity (neutral) state ($N_t^*$) (Fig.4b)

ii) the bound electron (negative) state ($N_t^-$) (Fig.4$c_1$ & $c_2$)

iii) the bound exciton state ($N_t^{ex}$). (Fig.4d).

Where the recombination parameters are given in table 1.

Recombination model in $GaAs_{1-x}P_x : N$

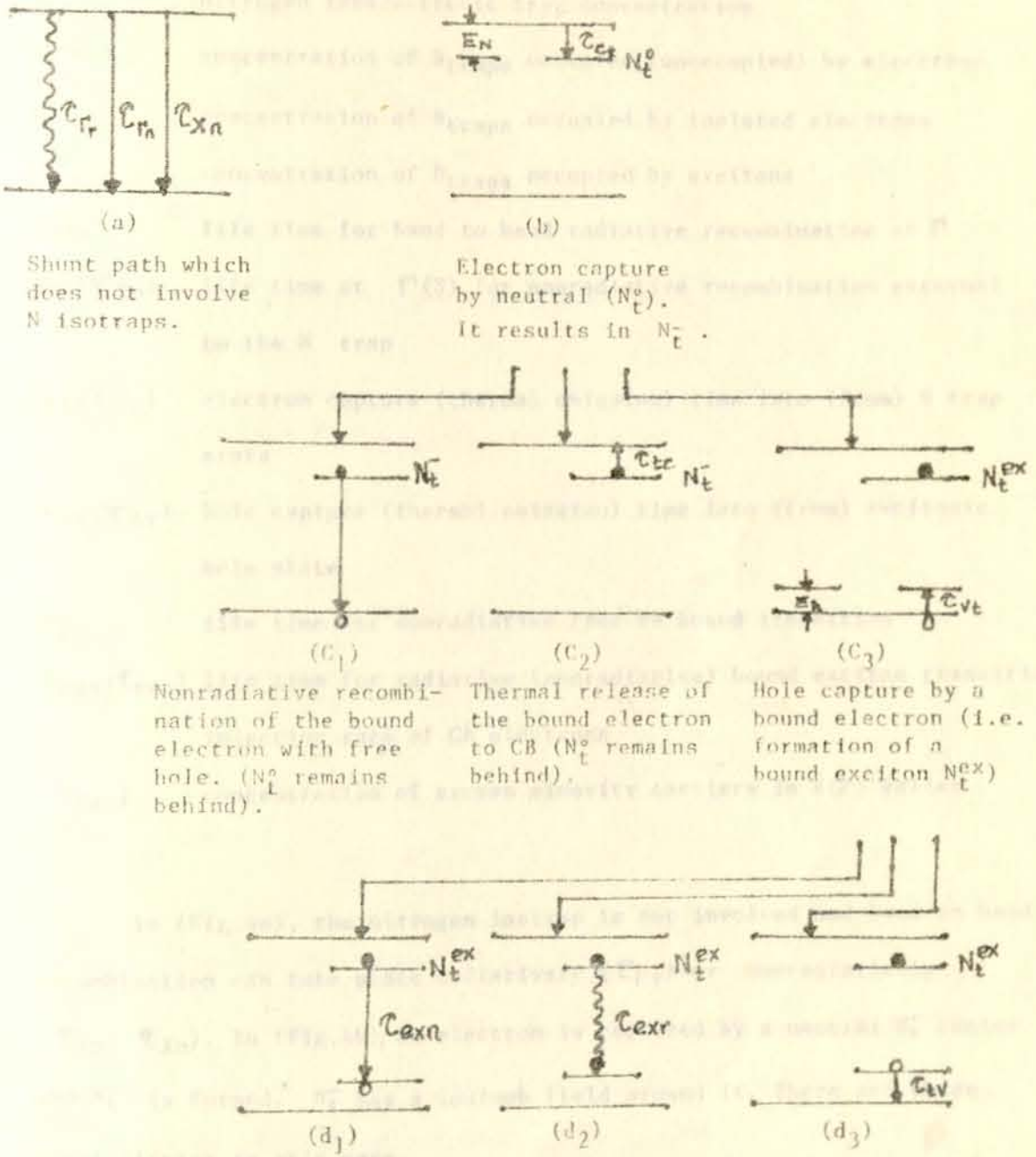


(a) Shunt path which does not involve N isotraps.

(b) Electron capture by neutral ($N_t^0$). It results in $N_t^-$.

($C_1$) Nonradiative recombination of the bound electron with free hole. ($N_t^0$ remains behind).

($C_2$) Thermal release of the bound electron to CB ($N_t^0$ remains behind).

($C_3$) Hole capture by a bound electron (i.e. formation of a bound exciton $N_t^{ex}$)

($d_1$) Nonradiative recombinations of bound exciton.

($d_2$) Radiative recombinations of bound exciton.

($d_3$) Dissociation of the bound hole. ($N_t^-$ remains behind).

Fig.4: Schematicrepresentation of electron hole recombination processes in $GaAs_{1-x}P_x : N$. [Adopted from Campbell et al[34]]. CB-conduction band.

Table 1 Recombination Parameters

| | |
|---|---|
| $N_t$ | nitrogen isoelectronic trap concentration |
| $N_t^e(N_t^\circ)$ | concentration of $N_t$ traps occupied (unoccupied) by electrons |
| $N_t^-$ | concentration of $N_t$ traps occupied by isolated electrons |
| $N_t^{ex}$ | concentration of $N_t$ traps occupied by excitons |
| $\tau_{\Gamma\Gamma r}$ | life time for band to band radiative recombination at $\Gamma$ |
| $\tau_{\Gamma n}(\tau_{Xn})$ | life time at $\Gamma(X)$ for nonradiative recombination external to the N trap |
| $\tau_{ct}(\tau_{tc})$ | electron capture (thermal emission) time into (from) N trap state |
| $\tau_{vt}(\tau_{tv})$ | hole capture (thermal emission) time into (from) excitonic hole state |
| $\tau_{en}$ | life time for nonradiative free to bound transition |
| $\tau_{exr}(\tau_{exn})$ | life time for radiative (nonradiative) bound exciton transition |
| G | injection rate of CB electrons |
| $n_X(n_\Gamma)$ | concentration of excess minority carriers in X($\Gamma$) valley. |

In (Fig.4a), the nitrogen isotrap is not involved and band to band recombination can take place radiatively ($\tau_{\Gamma\Gamma r}$) or nonradiatively ($\tau_{\Gamma n}$, $\tau_{Xn}$). In (Fig.4b), an electron is captured by a neutral $N_t^\circ$ center and $N_t^-$ is formed. $N_t^-$ has a Coulomb field around it. There are three possibilities in this case.

i) the electron may recombine nonradiatively with a hole ($\tau_{en}$)

ii) it may also be excited back to the conduction band leaving behind $N_t^\circ$ ($\tau_{tc}$) or

iii) it can attract a hole such that the hole assumes $E_h$ energy state ($\tau_{vt}$) and the two (i.e. the electron and the hole) form a bound exciton ($N_t^{ex}$).

Again, the bound exciton can decay nonradiatively ($\tau_{exn}$) or radiatively ($\tau_{exr}$) or the hole may dissociate and be excited back to the valence band ($\tau_{tv}$).

Referring to (Fig.4), the rate equations describing the recombination kinetics are given as;

$$(dn/dt) = G - [(n_r/\tau_{rn}) + (n_r/\tau_{rn}) + n_x/\tau_{xn} + [(n_r + n_x)/\tau_{ct}](1 - N_t^e/N_t) - (N_t^e - N_t^{ex})/\tau_{tc}] \quad (14a)$$

$$(dN_t^{ex}/dt) = (N_t^\circ - N_t^{ex})/\tau_{vt} - N_t^{ex}(1/\tau_{exn} + 1/\tau_{tv} + 1/\tau_{exr}) \quad (14b)$$

$$(dN_t^e/dt) = [(n_r + n_x)/\tau_{ct}](1 - N_t^e/N_t) - (N_t^e - N_t^{ex})(1/\tau_{tc}) - (1/\tau_{en}) - N_t^{ex}(1/\tau_{exn} + 1/\tau_{exr}) \quad (14c)$$

$$N_t^e = N_t^- + N_t^{ex} \quad (14d)$$

$1 - N_t^e/N_t$ gives the fraction of $N_t^\circ$ levels untrapped either by isolated electrons or by excitons. $(N_t^e - N_t^{ex})/\tau_{tc} = N_t^-/\tau_{tc}$ gives the fraction of electrons excited to the conduction band. $f = N_t^{ex}/N_t^e$ is the fraction of trapped electrons in exciton states which is equal to hole occupancy probability on an electron occupied N trap.

Using the assumptions that

i) at low excitation levels, excitonic holes are in thermal equilibrium with holes in the valence band & f is equal to the equilibrium hole occupancy probability.

ii) at low electron injection, $1-N_t^e/N_t \simeq 1$, since N traps are still far from being saturated.

iii) for low efficiency LEDs such as $GaAs_{1-x}P_x$, $\tau_{rr} >> \tau_{rn}$ & $\tau_{rr} >> \tau'_{xn}$: by at least an order of magnitude, $\tau_{rn} \simeq \tau_{xn} \simeq \tau_n$ and $1/\tau_{tc} + 1/\tau_{en} \simeq 1/\tau_{tc}$ holds for all crystal compositions. From steady state conditions and using the given assumptions;

$$G = (n_r/\tau_{rr}) + (n_r/\tau_{rn}) + (n_x/\tau_n) - (n_r+n_x)/\tau_{ct} - (N_t^e - N_t^{ex})/\tau_{tc}$$

$$= (n_r+n_x)\left[(1/\tau_n) + (1/\tau_{ct})\right] - (N_t^e - N_t^{ex})/\tau_{tc} \qquad (15a)$$

$$(N_t^e - N_t^{ex})/N_t^e = (N_t^{ex}/N_t^e)\left[(\tau_{vt}/\tau_{exn}) + (\tau_{vt}/\tau_{tv}) + (\tau_{vt}/\tau_{exr})\right]$$

$$f = \left[1 + (\tau_{vt}/\tau_{exn}) + (\tau_{vt}/\tau_{tv}) + (\tau_{vt}/\tau_{exr})\right]^{-1} \qquad (15b)$$

$$(n_r+n_x)/\tau_{ct} = (N_t^e - N_t^{ex})(1/\tau_{tc} + 1/\tau_{en}) - N_t^{ex}(1/\tau_{exn} + 1/\tau_{exr})$$

$$(n_r+n_x)/\tau_{ct} = N_t^e\left[(1-f)/\tau_{tc} - f(1/\tau_{exn} + 1/\tau_{exr})\right] \qquad (15c)$$

Internal quantum efficiency is defined as

$$\eta = \frac{\gamma(I_{out})}{I_{device}} = \gamma(dq\alpha/dt)/I_{device} \qquad (16a)$$

where $\alpha$ represents n or p, q is the electronic charge and $\gamma$ is a fraction of the output current that ends up in radiative recombination.

Therefore, $\gamma q\phi$ is the total number of carriers ending up in radiative recombinations.

$$\gamma d\phi/dt = R \quad \text{(Radiative recombination rate)}$$

Using R in eqn.(16a); yields

$$= q(d\phi/dt)/I = Rq/I \ , \ I = I_{device} \tag{16b}$$

In the presence of isoelectronic traps this internal efficiency could be taken as the sum of two terms; efficiency due to intrinsic transition ($\eta_\Gamma$) and efficiency due to transitions assisted by isoelectronic traps ($\eta_N$).

$$\eta = \eta_\Gamma + \eta_N = (\gamma/G)(n_\Gamma/\tau_{\Gamma r}) + (\gamma/G)(N_t^{ex}/\tau_{exr})$$

$$= (\gamma/G)(n_\Gamma/\tau_{\Gamma r} + N_t^{ex}/\tau_{exr}) \tag{16c}$$

Using equations (15a) and (15b) in (16c) yields,

$$\eta_\Gamma = \gamma[(n_\Gamma+n_x)/(1/\tau_n + 1/\tau_{ct}) - (N_t^e-N_t^{ex})/\tau_{tc}]^{-1}(n_\Gamma/\tau_{\Gamma r})$$

$$= \gamma(1+n_x/n_\Gamma)(\tau_{\Gamma r}/\tau_n)+[(1+n_x/n_\Gamma)(\tau_{\Gamma r}/\tau_{ct}) -$$

$$- (N_t^e-N_t^{ex})/n_\Gamma\,(\tau_{\Gamma r}/\tau_{tc})]^{-1} \tag{17a}$$

$$\eta_N = \gamma[(n_\Gamma+n_x)(1/\tau_n+1/\tau_{ct}) - (N_t^e-N_t^{ex})/\tau_{tc}]^{-1}\,(N_t^{ex}/\tau_{exr})$$

$$= \gamma[(1+\tau_{exr}/\tau_{exn})(1+\tau_{ct}/\tau_{xn}) + (1/f-1)(\tau_{ct}/\tau_{tc})(\tau_{exr}/\tau_{xn})]^{-1} \tag{17b}$$

The term $1+(n_x/n_\Gamma)(\tau_{\Gamma r}/\tau_n) = [(n_x+n_\Gamma)/\tau_n](\tau_{\Gamma r}/n_\Gamma)$ in (17a) is an expression obtained for the quantum efficiency of a ternary alloy in the absence of N trap. The reciprocal of this value gives the ratio of radiative over nonradiative processes. The remaining term shows the effect

of N trap in reducing $\eta_{\Gamma}$ . This indicates the negative effect of N trap on efficiency in the direct gap region where $\eta_{\Gamma}$ plays the major role.

In $\eta_N$, there are two terms at the dinominator; $(\tau_{exn}+\tau_{exr})(\tau_{xn}+\tau_{ct})/(\tau_{exn}\tau_{xn})$ and $(N_t{}^{e}+N_t{}^{ex})(\tau_{ct}\tau_{exn})/(N_t{}^{ex}\tau_{tc}\tau_{xn})$. The efficiency $\eta_N$ is basically dependent on the nonradiative lifetimes $\tau_{exn}$ and $\tau_{xn}$.

### 1.3.3 Minority Carrier Lifetime

Minority carrier lifetime is defined as the time it takes the excess minority carrier density to decay to 1/e of its initial value. The duration of emission is determined by the time the carriers spend in the traps. An increase in minority carrier lifetime would indicate an increase in efficiency of EL diodes. High carrier concentration which is characterized by free exciton, Auger and other nonradiative recombinations reduces minority carrier lifetimes[39].

The recombination rate in the depletion layer is controlled by the separation of the quasi Fermi levels which in turn is determined by the majority carrier concentration and the applied voltage. Recombination in the diffusion region on the other hand is governed by the lifetime of the injected minority carriers; a parameter which is much more defect - sensitive[40].

The efficiency of Ga (As,P) EL diodes have been characterized by the nitrogen concentrations, minority carrier lifetimes of both carriers and majority carrier concentrations or doping levels $(N_D-N_A)$ particularly

in the indirect region. In indirect gap semiconductor, the minority carrier lifetime is relatively long and hence long diffusion lengths are required in efficient material[39].

## 1.4 NONRADIATIVE RECOMBINATIONS

### 1.4.1 Defects and Deep Impurity Levels

Defects in crystals introduce additional energy states in the energy gap and thus, additional extrinsic electrical and optical properties are manifested. The defects can be point defects such as the one caused by substitutional or interstitial impurities or line defects as dislocations. Be it intentional or unintentional, impurities which occupy deep level states are one of the major areas where nonradiative recombinations take place. Such defects can be caused by[41]

i) discontinuities in the lattice constant at the interface between the substrate and the epitaxial layer (i.e. lattice mismatch)

ii) difference in thermal construction to compounds (say GaP & GaAs) on cooling from growth temperature (i.e. difference in thermal expansion coefficient).

Deep states are not ionized at room temperatures. Relatively small concentrations of such states can compete with shallow activators such as N isotraps because of the much greater thermal re-emission rates of the activators. They, therefore, provide an alternative (shunt) path for the minority carriers injected into the EL diode. Sometimes, the cross-

sections of the deep centers can be very small but they can be greatly augmented by the effects of large lattice deformations such as dislocations which act as an efficient energy loss.

Nonradiative surface recombination can also be the cause for efficiency loss. It can occur when a continuum or quasi continuum states join the conduction band to the valence band. Such surface recombinations may be enhanced by pores, grain boundaries and dislocations.

As deep trap density decreases, EL efficiency increases since space charge recombination current decreases and the electron diffusion length increases thereby allowing injected minority carriers to penetrate deeper into the luminescence material[42]. EL diodes radiant output also decreases as junction temperatures increase. This implies that as temperature increases, most of the recombination processes would be nonradiative.

High doping ($\sim 10^{19}/cm^3$) introduces precipitates and causes line widening (since at high doping or high excitation the conduction band population increases and the spectrum is shifted) and reduces efficiency. It also produces tunneling break down at relatively low voltages[43].

### 1.4.2 Auger Recombinations

When an electron transfers from the conduction band to some lower energy state, it may radiate photons (radiative process) or phonons or it may transfer its energy to another free electron or hole (nonradiative process). The last process is referred to as an Auger process.

An Auger process is an example of an intrinsic nonradiative process. Such a process is present as a consequence of the density of free carriers in the region of the semiconductor where the radiative recombination occurs. Auger process can arise as a result of high doping. The effect of Auger recombination on internal efficiency in moderately doped semiconductors with wide band gaps is not large. It is insignificant in indirect gapped semiconductors.

Auger recombination can take place for bound excitons at neutral donors or it can also involve free carriers. In such an Auger recombination, all of the exciton transition energy appears as kinetic energy of one of the particles. It may occur even for excitons bound to isoelectronic traps if a mechanism exists whereby a third electronic particle can interact with the bound exciton[44].

## 1.5 DEGRADATION IN EL DIODES

Degradation is efficiency loss that is observed in EL diodes as a function of operation time. LEDs, unlike other light sources have a merit such that before complete failure is observed intensity loss is manifested. This efficiency loss can be caused by surface contamination or by bulk phenomena.

The main reason för an efficiency loss in EL diodes is due to current stress under forward bias (i.e. bulk phenomena). The forward bias brings about two effects on the EL diodes[45].

i) As a result of the bias, field aided diffusion is observed along the dislocation lines.

ii) An additional mechanical effect associated with a large thermal gradient near the active layer is also observed. Junction heating in LEDs brings about thermal expansion which is sufficient to generate lattice defects in a uniform material.

Generation of defect centers in the course of operation is a gradual process. Progression of multiplication of lattice defects is observed once a defect is formed due to the effective shear stress acting on the dislocation[46]. The effect of such defects is more pronounced if they are introduced within diffusion length of the p-n junction since radiative recombination occurs within this length[47].

It may happen that through time excess concentration of dopants may arise in the recombination region or out of tolerance variation of concentration of intentional dopants may be observed. In addition, surface flows due to mechanical damage in handling or chemical contamination can also bring about degradation. The degradation rate is high for increasing energy gap within a series of semiconductor alloys. It is also accelerated by small particle size, higher firing and higher operating temperatures[48].

Unlike radiation damage, thermal annealing can not remove degradation caused by current effect[47,49]. Thus, degradation due to bulk phenomena is permanent whereas degradation caused by surface effects may be improved by chemical etching.

# II MATERIALS AND METHODS OF MEASUREMENT

In this chapter, the samples are specified and instruments and experimental procedures are described. The main purpose of this work was to study all possible electrical and optical properties of EL diodes. During the work a wide spectrum of parameters of EL diodes were determined. An attempt was made to correlate some of these parameters.

## 2.1 Sample Specification

There were two sets of EL diodes available for the experimental study. In the first set, there were four groups each with seven samples. These EL diodes were made by TESLA ELECTRONICS, Czechoslovakia and they were identified as RED (LQ1131), labeled, $R_1$, $R_2$, $R_3$, $R_4$, $R_5$, $R_6$, $R_7$; ORANGE (Unidentified experimental samples without catalogue number), labeled $O_1$, $O_2$, $O_3$, $O_4$, $O_5$, $O_6$, $O_7$; YELLOW I (LQ 1431), labeled $Y_1$, $Y_2$, $Y_3$, $Y_4$, $Y_5$, $Y_6$, $Y_7$ and GREEN I (LQ 1731), labeled, $G_1$, $G_2$, $G_3$, $G_4$, $G_5$, $G_6$, $G_7$.

In the second set, there were two groups of EL diodes consisting of three smaples each. These samples were made by RADIO SPARES (RS), England and were identified as:

YELLOW II ($LED_4$-586-497), labeled $y_1$, $y_2$, $y_3$, and

GREEN II ($LED_4$-586-481), labeled, $g_1$, $g_2$, $g_3$.

Electrical and optical studies and band gap measurements were carried out for each of the 34 samples independently. As to the electrical properties, I-V and C-V characteristics studies were made at forward and reverse bias, respectively. Optical properties were studied by emission and luminosity measurements. Finally, thermal band gap measurements were made.

## 2.2 Electrical Measurements

1) I-V measurements were taken at room temperatures within voltage ranges from 0.0 to ~2.5 volts. Stablized 6205B dual dc Hewlett Packard (HP) power supply was used to bias the diodes. PM 2517E Philips digital voltmeter (of 10MΩ internal resistance, 2% accuracy and 1mV resolution) and MA 4E Leybold Heraeus (LH) analog multimeter (of 10 MΩ internal resistance, 1.5% accuracy and 0.01 nA resolution) were used for voltage and current measurements, respectively. Experimental setup for the I-V measurement is shown in Fig.5. An attempt to study I-V characteristics under reverse bias has failed since the reverse current was below the resolution power of the MA4E multimeter.

Temperature readings were taken during I-V measurements of each diode. Evaluation of the ideality factor n was made from the slope of the linear region of $\ln I$ vs V graph. Curve fitting was done by the least square regression method using TI-59 programmable calculator. Plots of I-V characteristics for representative samples of each group are given in Fig.9 and mean values of ideality factors in table 2.

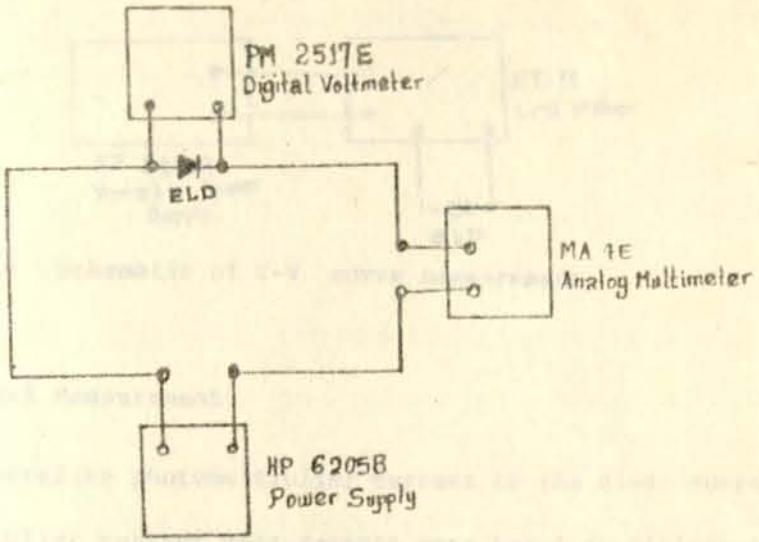


Fig.5: Schematic Diagram for I-V curve measurement. ELD stands for electroluminescent diode.

ii) C-V characteristics studies were made for each diode using E7-11 (USSR) LCR meter (of an accuracy better than 1OZ) at a frequency of 100Hz. The diodes were reverse biased using HP 6205B power supply. Voltage readings were taken using PM 2517E multimeter at intervals of 0.1V over the voltage range from 0-4.8 volts. The setup is shown in Fig.6. The capacitance, as mentioned in the theory part is related to the voltage as $C \sim V^{-\frac{1}{2}}$ for an abrupt junction . Plots of $1/C^2$ vs V were made for each group. Curve fittings were again made using the least square method. Concentrations of the smaller of the impurities ($N_D$ or $N_A$) and built in potentials ($V_{bi}$) were determined from the slopes and the intercepts, respectively.

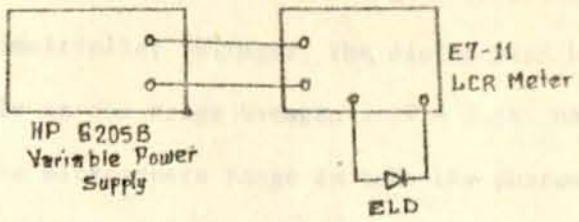


Fig.6: Schematic of C-V curve measurement.

2.3 Optical Measurement

1) To correlate photomultiplier current to the diode current, photomultiplier current measurements were taken at different diode bias. For this, the diode was kept in a confined box where no measurable amount of light could enter from the surroundings. A hole with the dimension of the diode was made on one side of the box. The light from the diode was directed to ФЭУ-79 (USSR) photomultiplier (which has a maximum sensitivity range between 400 - 440 nm) through this hole. The photomultiplier was biased by a 2K 369 5KV Philip Harris dc power supply. Care was taken to keep every diode at the same orientation and at the same distance from the photomultiplier every time. The experimental arrangement is shown in Fig.7.

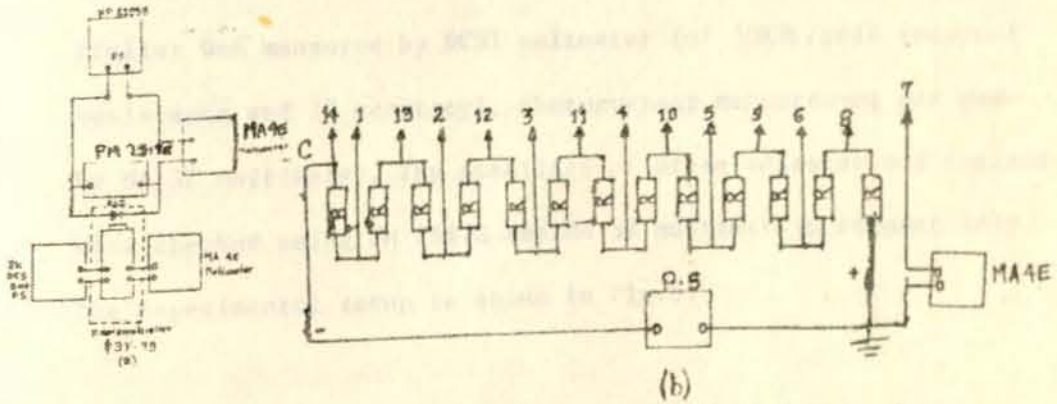


Fig.7: (a) Schematic diagram for luminosity measurements. (b) Components of the photomultiplier. Dashed lines indicate dark box.

Photomultiplier current readings were taken at 1000V and 2000V photomultiplier voltages. The diodes were biased by 6205B power supply in the range between 1.2V - 2.5V. MA 4E multimeter was used in the microampere range to take the photomultiplier current readings. PM 2517E and MA 3E Leybold Heraeus multimeter (of 10MΩ internal resistance and 1.5% accuracy) were used to measure diode voltages and currents, respectively. The natural logarithm of photomultiplier current and diode current were taken and plotted against diode voltage and comparisons of the dependence of both currents on voltage were made. This, in our laboratory was the nearest substitute to study LIV (Luminosity and current versus voltage) characteristics.

ii) Study of the emission spectra of each group of EL diodes was made using 60741 Hilger Constant Deviation spectrometer and ΦЭУ - 79 photomultiplier. The photomultiplier was biased by two 52237 Leybold Heraeus High Voltage dc power supplies connected in series to get an output of 2300V. It allowed to read maximum sensitivity of the photomultiplier. The voltage of the photomultiplier was measured by DCHI voltmeter (of 50KΩ/volt internal resistance and 1% accuracy). Photocurrent measurement was made by MA 3E multimeter. The stability of diode voltages and currents were checked using PM 2517E and MA 3E multimeters, respectively. The experimental setup is shown in Fig.8.

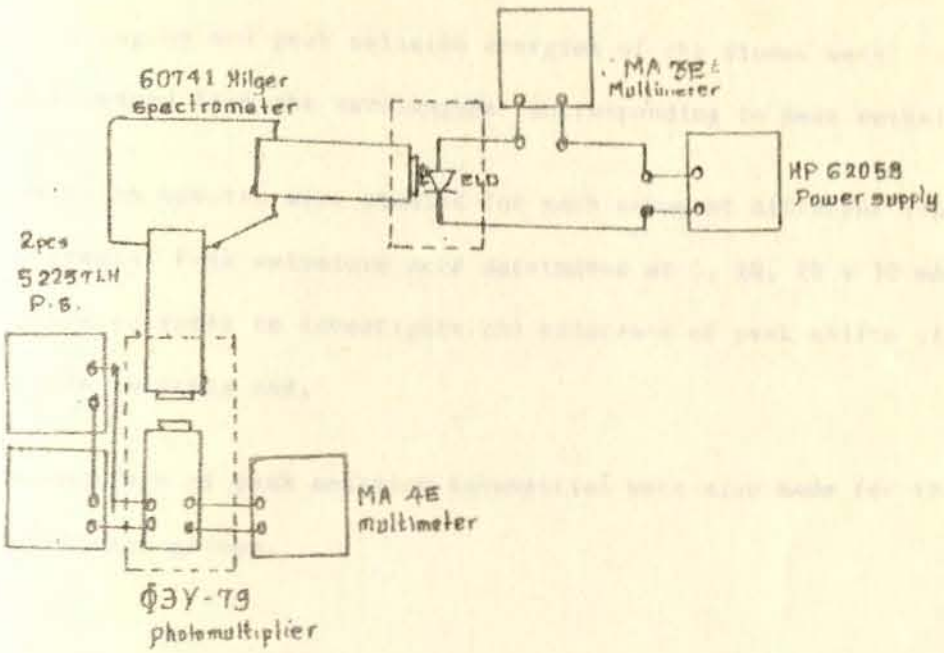


Fig.8: Spectral Characteristics Measurements. Dark lines indicate regions protected against light from the surroundings.

Before taking readings, the calibration of the spectrometer was checked by a sodium discharge lamp. Necessary calibration was done for the photomultiplier spectral response as is given in the correction curve of Fig.13. Since the light emitted from each diode was small and a slight external light could affect the spectrum, much care was taken to control the effect of the external sources. Correction was made for light due to digital meters and indicator lamps. Finally, readings of

photomultiplier current against wavelength were taken by varying the wavelength and keeping the diode voltage constant. In this particular case;

a) wavelengths and peak emission energies of the diodes were determined from the wavelengths corresponding to peak emissions,

b) emission spectra were studied for each group at different diode currents. Peak emissions were determined at 5, 10, 20 & 30 mA diode currents to investigate the existence of peak shifts with diode currents and,

c) comparison of peak emission intensities were also made for the different groups.

## 2.4 Thermal Band Gap Measurement

In this experimental work, a final attempt was made to determine thermal band gap of each diode. For this, due to lack of thermostat, 102 Fisher oven was used. In addition, because of low sensitivity of the meters, it was not possible to carry out this particular experiment with the diodes under reverse bias. Rather, mean voltages at which the ideality factors (n) in ($I = \exp(qV/nKT)$) assumed constant values (i.e. 1.6V for green and yellow, 1.7V for orange and 1.4V for red EL diodes) were chosen to bias the diodes at constant voltages. The voltages for each EL diode were checked by 3478A Hewlett Packard multimeter (of 100nV resolution and input resistance exceeding $10^{10}\Omega$) to four significant figures. Seventeen EL diodes were fixed to a circuit board and placed in a horizontal position

in the oven (to minimize the effect of temperature gradient) at a time and the diodes were heated upto a temperature of 70°C. This temperature was the maximum limit for the EL diodes used in the experiment. Simultaneous current and temperature readings were taken for each diode in the process of cooling. MA 3E multimeter was used for current measurement. Temperature readings were taken with a thermometer which had a range from - 5°C to 100°C and 0.2°C resolution. Readings were taken from 70°C down to room temperature at intervals of about 5°C. From the readings, $\ln I$ vs $(1/T)$ was plotted and energy gaps ($E_g$) were determined from the slopes.

## III EXPERIMENTAL RESULTS AND DISCUSSION

Based on the measurement procedures described in the previous sections, the results obtained are presented in this chapter.

### 3.1 I-V Characteristics

The I-V characteristics study reveals that there exists a linear region in the $\ell n I$ vs V curve (Fig.9) which extends over about two decades of voltage (1.5V - 1.7V) for most of the diodes except the red ones. In red EL diodes however, the linear region extends over about four decades (1.2 - 1.6V).

The mean values of ideality factors for each group evaluated from the slopes of the linear regions by curve fitting are given in table 2.

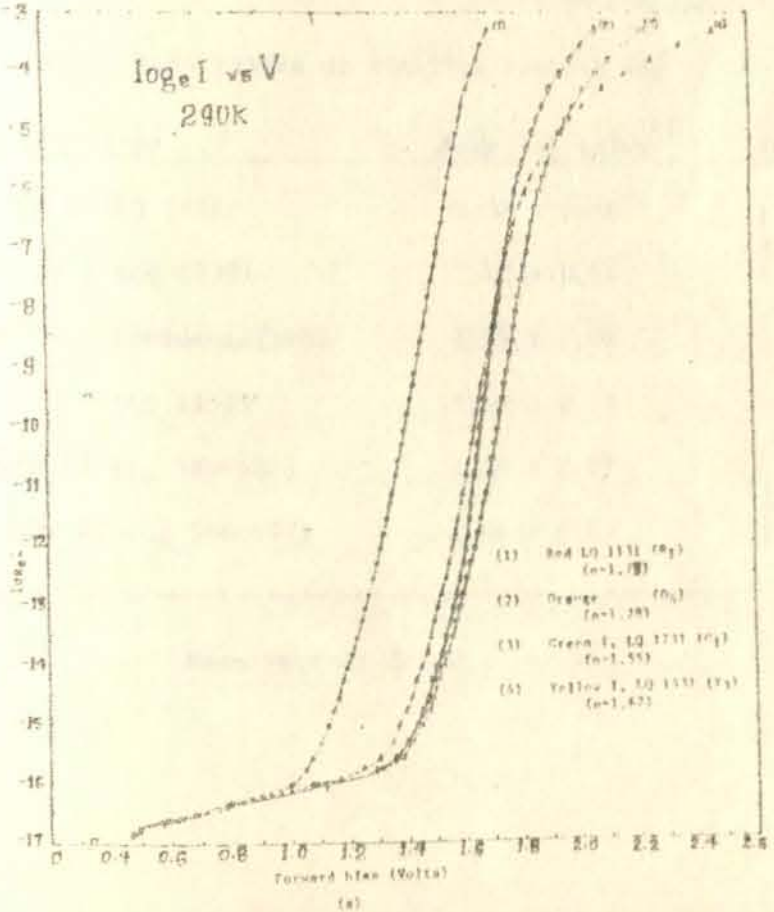


(a)

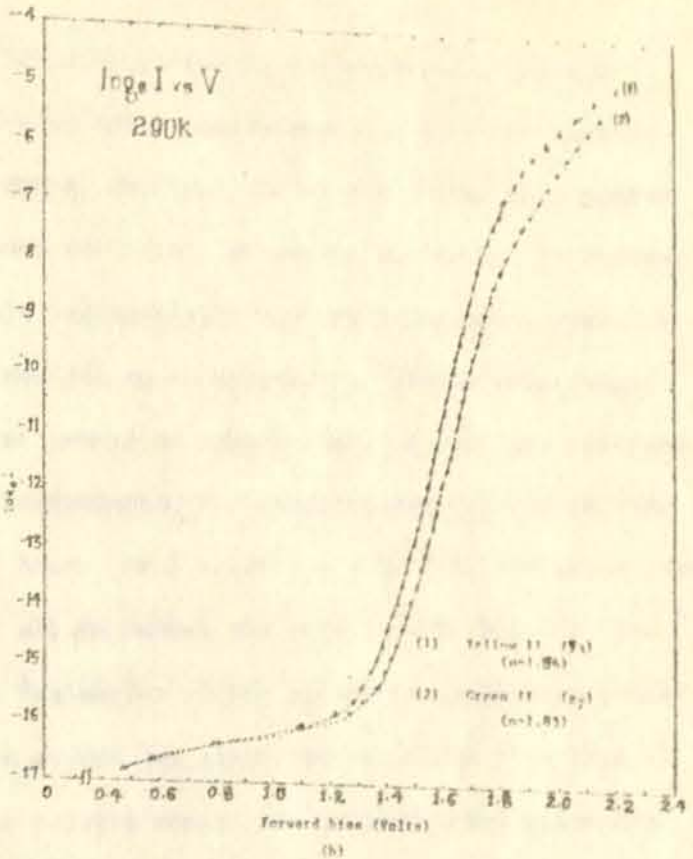


Fig.9: I-V characteristics of the representative samples from the first set (a) and the second set (b) of EL diodes under forward bias. The samples were selected on the basis of their ideality factors which are closer to the mean values of their respective groups.

Table 2. Mean Values of Ideality Factors (n)

| LED Type | Mean 'n' Value | Voltage Range (V) |
|---|---|---|
| GREEN I (LQ 1731) | 1.53 ± 0.16 | 1.5 - 1.7 |
| YELLOW I (LQ 1431) | 1.65 ± 0.06 | |
| ORANGE (unidentified) | 1.29 ± 0.02 | 1.6 - 1.8 |
| RED (LQ 1131) | 1.74 ± 0.12 | 1.2 - 1.6 |
| GREEN II ($L_4$ 586-481) | 1.94 ± 0.07 | 1.5 - 1.7 |
| YELLOW II ($L_4$ 586-497) | 1.84 ± 0.06 | |

Mean Percent Error ~ 6%

The values of the ideality factor range between 1.0 and 2.0 indicating that both diffusion and recombination currents are present within the given voltage range. In Fig.9 all of the curves have almost constant slopes below 1 volt (or $< 10^{-7}$ A) except in the red EL diodes. The ideality factor in this region highly exceeds 2 and the current is neither due to diffusion nor due to recombination. Within this range, the current is also not influenced by temperature. At such low voltages, the current is basically predominated by tunneling and this is in line with the work of Shih[50]. Above ~1.8 volts ($\sim > 10^{-7}$ A) deviation from linearity is observed for all the curves and this is attributed to the series resistance effect. Evaluation of the series resistance values by extrapolation for all the diodes has given values within the range of 5 - 25 Ω . However, these results should not be considered since high injection current might have also an effect in this region. The result shows an agreement at least in the order of magnitude with the ~10Ω resistance obtained by others[51,43]. High series resistance indicates low injection effeciency, It also affects the light emission efficiency in the region where the series resistance has substantial influence.

Comparison of ideality factor values within the first four groups shows domination of diffusion currents in orange EL diodes with $n \simeq 1.3$ as compared to red EL diodes with $n \simeq 1.7$ in which recombination currents have greater influence. Comparison of the two sets indicate early and strong series resistance effects in the second set (i.e. RS EL diode).

3.2 C-V Characteristics

The linear plots of $(1/C^2)$ against the reverse bias are shown for six representative samples of each group (Fig.10). As observed from the value of the correlation coefficient, the lines fit into the data points very well. The linearity in all the EL diodes indicate that the junctions are abrupt. Extrapolation of the curve to $1/C^2 = 0$ (i.e. the intercept) gives $V_{bi} - 2KT/q$. Hence, the value of the built in potential ($V_{bi}$) at a given temperature is obtained for each EL diode from the intercept.

Concentration of the smaller of donors ($N_D$) or acceptors ($N_A$) could be obtained from the slopes as follows.

$$\partial(1/C^2)/\partial V = 2/(q \varepsilon_s N_B)$$

$$N_B = 2/q\varepsilon_s [\partial(1/C^2)/\partial V] \qquad (10b)$$

$$\varepsilon_s = \varepsilon_0 \varepsilon_r \quad \text{where} \quad \varepsilon_0 = 8.85418\times10^{-14}\text{F/cm}$$

The ratio of the permitivity of the semiconductor to that of the vacuum ($\varepsilon_s/\varepsilon_0$) could be obtained from the value for Ga As ($\varepsilon_s/\varepsilon_0 = 13.1$) and Ga P ($\varepsilon_s/\varepsilon_0 = 11.1$)[52]. To evaluate $\varepsilon_s/\varepsilon_0$ for the EL diodes used in the experiment two basic assumptions were made.

i) that all the EL diodes are made from $GaAs_{1-x}P_x$ ternary alloys;

ii) $\varepsilon_s/\varepsilon_0$ value changes depending upon the variation in the composition of $A_sP$.

Starting with the difference of $\varepsilon_s/\varepsilon_0$, ($\Delta(\varepsilon_s/\varepsilon_0)$) of the two binary compounds,

$$\Delta(\varepsilon_s/\varepsilon_0) = 13.1 - 11.1 = 2.$$

Taking Ga $As_{0.6}$ $P_{0.4}$ (red) for instance, one can assume that this EL diode consists of 60% Ga As and 40% Ga P. Thus, its $\varepsilon_s/\varepsilon_o$ value is given by $\varepsilon_s/\varepsilon_o$ (red) = 13.1 - (2x40/100)=11.1 + (2x60/100) = 12.3

By the same analogy, evaluation for Ga $As_{0.35}$ $P_{0.65}$ and Ga $As_{0.15}$ $P_{0.85}$ yields 11.8 and 11.4, respectively.

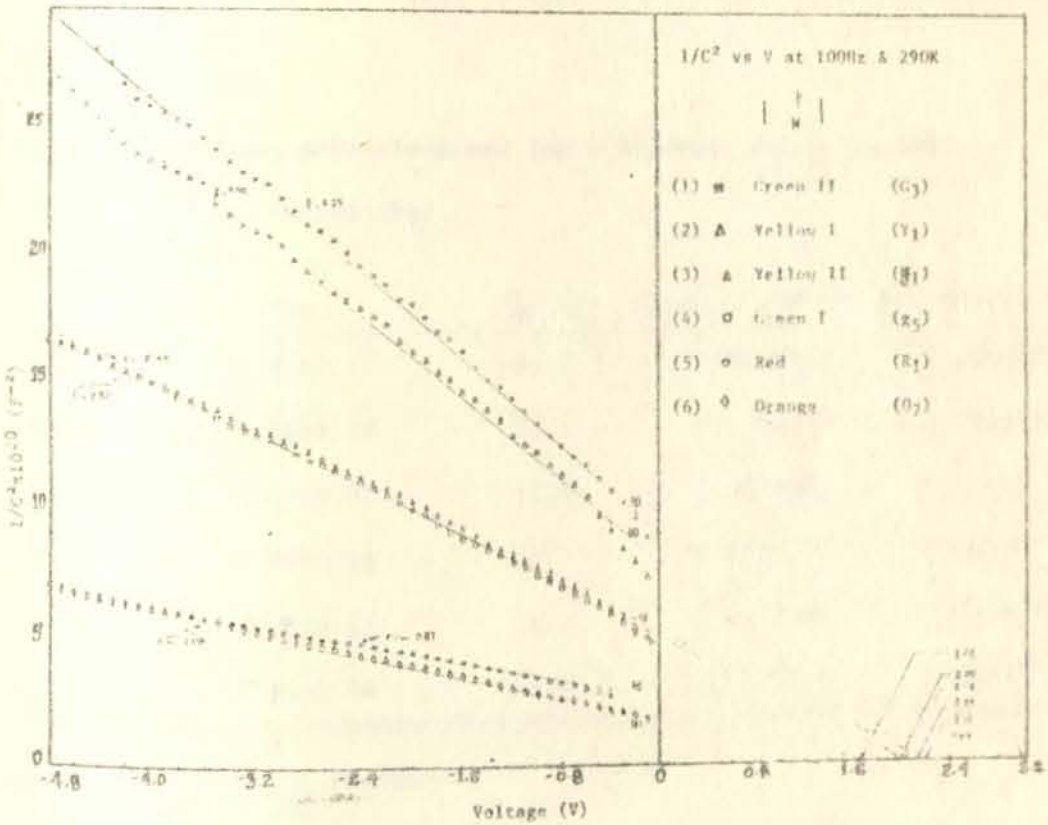


Fig.10: C-V characteristics of 6 representative samples of each group at 100Hz and 290K. The straight lines indicate best fits to the data points. Intercepts and slopes are shown for the six samples.

The capacitance values measured in the experiment represent the capacitance of the entire junction. To evaluate $N_B$, the value of capacitance per unit area is necessary. However, in the experiment, the area of the junction could not be determined precisely. Rather, inorder to get a rough estimate of $N_B$, junction area of $10^{-3}$ cm$^2$ was taken as a fair estimation[50]. The slopes are evaluated by taking the junction area into account and by making use of the already obtained $\varepsilon_s$ values. Then, values of $N_B$ are computed. The results obtained are summarized in table 3.

Table 3. Built-in potentials and the less dense donor (or acceptor) concentration ($N_B$)

| LED Color | $V_{bi}$ | $\varepsilon_s/\varepsilon_o$ | Slope($\times 10^{20} F^{-2} V^{-1}$) | $N_B/cm^3$ |
|---|---|---|---|---|
| GREEN I | 1.92±0.11 | 11.1 | 2.53±0.34 | $5.0\times10^{16}$ |
| YELLOW I | 2.04±0.18 | 11.4 | 4.25±1.52 | $2.9\times10^{16}$ |
| ORANGE | 1.63±0.02 | 11.8 | 1.06±0.08 | $1.1\times10^{17}$ |
| RED | 2.89±0.18 | 12.3 | 0.87±0.14 | $1.3\times10^{17}$ |
| GREEN II | 2.06±0.12 | 11.1 | 4.63±1.09 | $2.7\times10^{16}$ |
| YELLOW II | 2.14±0.04 | 11.4 | 2.12±0.50 | $5.8\times10^{16}$ |

Percent Error $\sim 5\%$

As seen from the table, $N_B \sim 10^{17}/cm^2 < 10^{19}/cm^2$ indicating that at least one side of the EL diode is nondegenerate. Built-in potentials ranging between 1 and 3 volts are observed in this work. Similar results were obtained in other p-n junctions[53] and Schottky barrier [illegible].

In Fig.10 slight deviations of the data points from the linear curve are observed near V = 0. This shows that the EL diodes have variable $N_A - N_D$ concentrations near the junction. It is attributed to the presence of deep states which contribute to the capacitance when mobile carriers are present in the depletion region[53]. The deviation is more pronounced in Green II and Yellow I EL diodes which are characterized by decreased $N_B$ values in this particular experiment.

## 3.3 The Relationship of Photocurrent to Diode Voltage

Luminosity $\sim$ Iradiative $\sim$ Iphotomultiplier

The behavior of a photomultiplier current directly reflects the nature of the luminosity of the EL diodes. In EL diodes, within a voltage range under which diode current has an exponential dependence on voltage, the natural logarithm of photocurrent plotted against voltage would show linear behavior. However, the n' value in this case is different from the ideality factor n. The relationship between Iphoto and diode voltage is given in Fig.11 and n' values corresponding to the linear region of the curves are given in table 4.

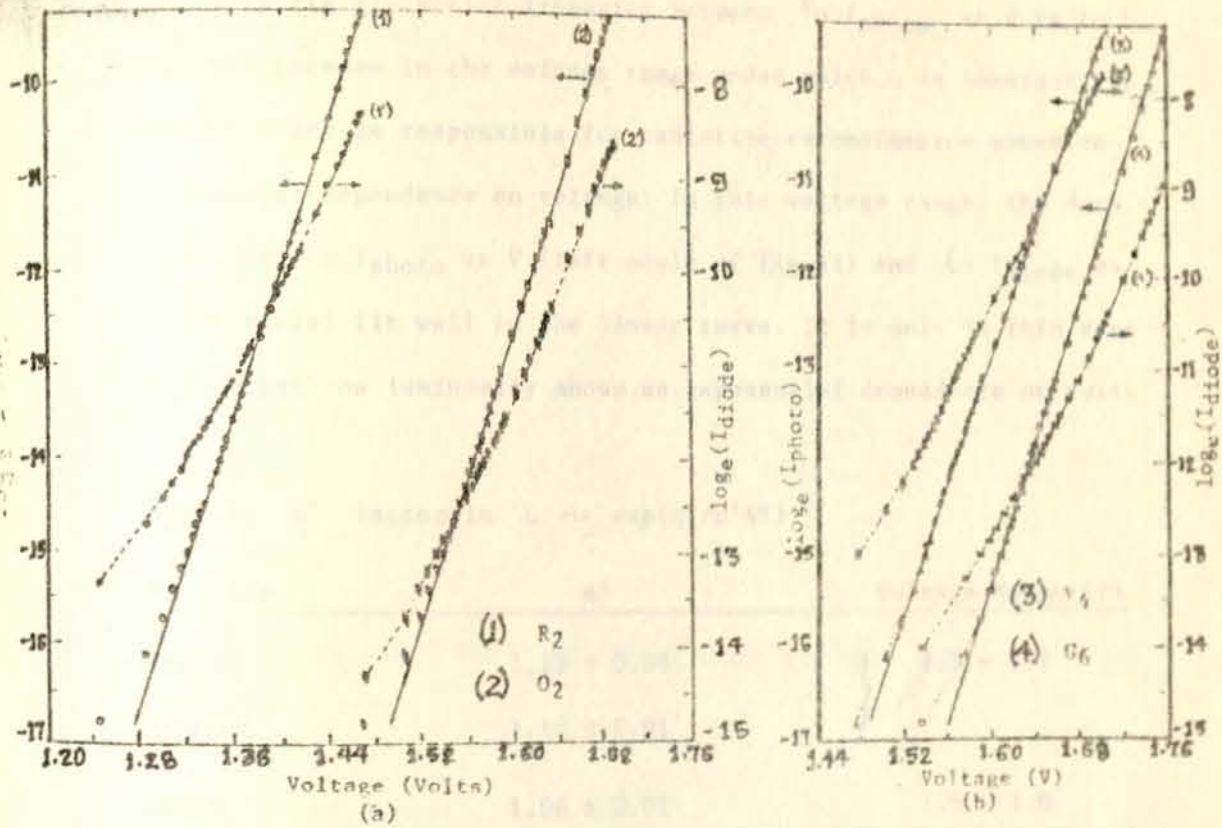


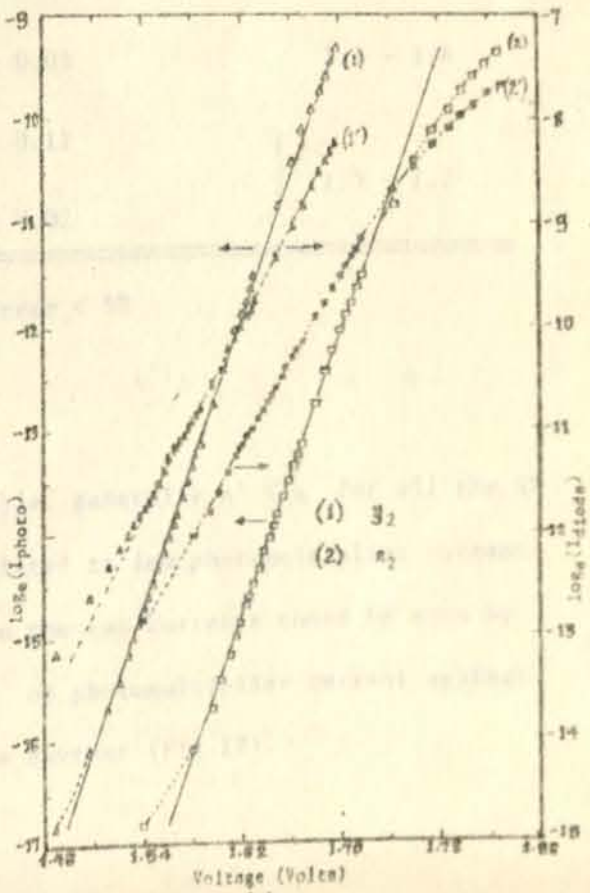


Fig.11: Photomultiplier current and Diode current against voltage at room temperature and photo-multiplier voltage of 2000V.

a) Red (1,1') and Orange (2 ,2')

b) Yellow I (3,3') and Green I (4,4')

c) Yellow II (1,1') and Green II (2,2')

In Fig.11, strict linearity between $\ln I_{photo}$ vs V is to b expected because in the voltage range under which n is constant, the current which is responsible for radiative recombination shows an exponential dependence on voltage. In this voltage range, the data points of $\ln I_{photo}$ vs V (left scale of Fig.11) and $\ln I_{diode}$ vs (right scale) fit well to the linear curve. It is only in this same region that the luminosity shows an exponential dependence on volta

Table 4. n' factor in $L \sim \exp(qV/n'KT)$

| LED color | n' | Voltage Range (V) |
|---|---|---|
| GREEN I | 1.13 ± 0.08 | 1.5 - 1.7 |
| YELLOW I | 1.18 ± 0.01 | |
| ORANGE | 1.06 ± 0.01 | 1.6 - 1.8 |
| RED | 1.09 ± 0.03 | 1.2 - 1.6 |
| GREEN II | 1.29 ± 0.12 | 1.5 - 1.7 |
| YELLOW II | 1.13 ± 0.02 | |

Mean Percent Error < 5%

As observed from the table, generally $n' < n$ for all the EI diodes. High n' value is correlated to low photomultiplier current. The actual relationship between the two currents could be seen by plotting the natural logarithm of photomultiplier current against the natural logarithm of diode current (Fig.12).

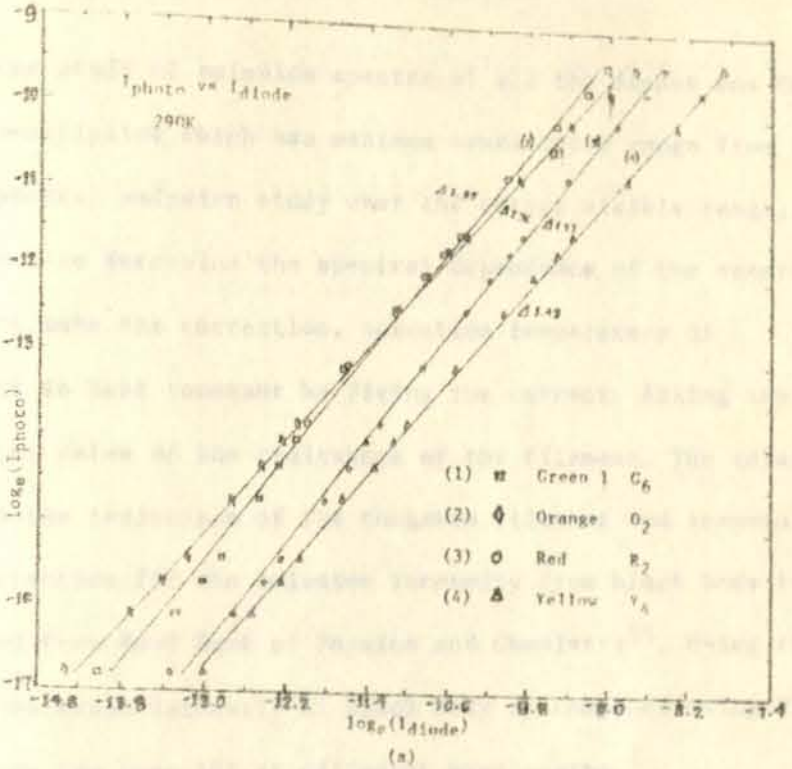


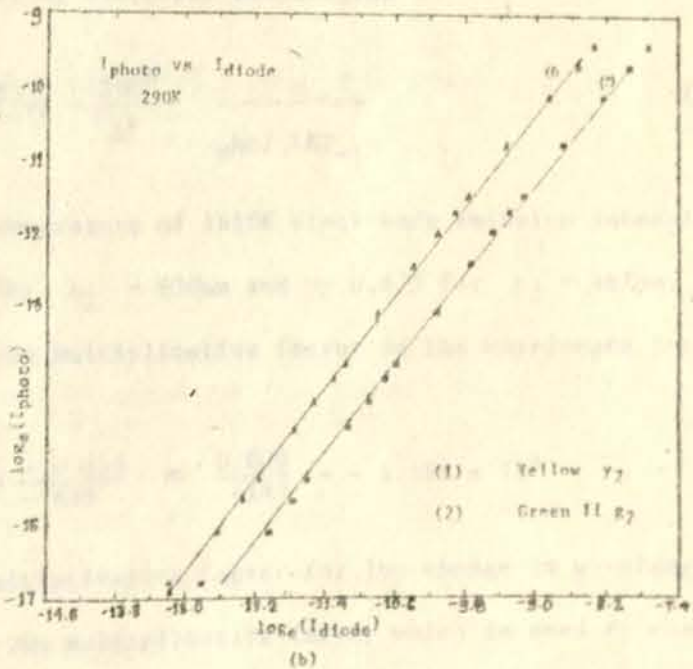


Fig.12: Comparison of photocurrent against diode current for photomultiplier voltage of 2000V.

a) 1st set

b) 2nd set

Here the slopes give the relative efficiencies of the EL diodes and they serve for comparison purposes. Red EL diodes have maximum efficiency as they ought to be due to their direct band gap.

## 3.4 Electroluminescence Emission Spectra

The study of emission spectra of all the diodes was carried out by a photomultiplier which has maximum sensitivity range from 400-440nm. To make spectral emission study over the entire visible range, it was necessary to determine the spectral dependence of the sensitivity. In order to make the correction, operation temperature of tungsten filament is kept constant by fixing the current. Fixing the current fixes the value of the resistance of the filament. The relationship between the resistance of the tungsten filament and temperature along with the correction for the emission intensity from black body to tungsten is obtained from Hand Book of Physics and Chemistry[55]. Using this temperature value, emission intensity of black body is computed using Planck's radiation law (eqn.18) at different wavelengths

$$\mathcal{E}(\lambda) = \frac{2\pi C^2}{\lambda^5} \frac{h}{e^{hc/\lambda KT} - 1} \qquad (18)$$

For instance, at a temperature of 1610K black body emission intensity is multiplied by 0.446 for $\lambda_1$ = 650nm and by 0.475 for $\lambda_2$ = 467nm. Assuming uniform decrease in the multiplicative factor as the wavelength increases, we get

$$\frac{0.475 - 0.446}{467 - 650} = \frac{0.029}{-183} = -1.585 \times 10^{4}$$

as a change in the multiplicative factor for 1nm change in wavelength. Thus, for $\lambda$ = 468nm, the multiplicative factor which is used to change $\mathcal{E}(\lambda)$ of black body to $\mathcal{E}(\lambda)$ of tungsten is $0.475 - 1.585 \times 10^{-4} = 0.4748415$. Emission intensity of tungsten is obtained from the emission intensity of black body following the foregoing procedure. Finally, correction factor is obtained for the photomultiplier as

$$\text{Correction Factor } (C\mathcal{E}(\lambda)) = \frac{\mathcal{E}(\lambda)\text{tungsten (theoretical)}}{I_{photo}(\lambda)\text{tungsten}} \qquad (19)$$

Based on this evaluation, the following correction factor curve is obtained for the ΦEMI Y - 79 photomultiplier at its operating voltage of 2300V.

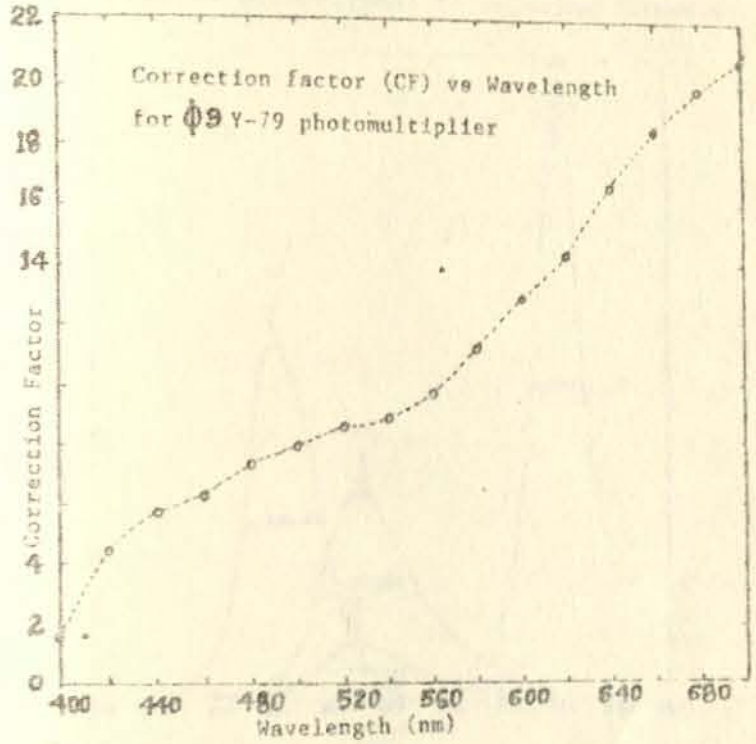


Fig.13: Correction factor for ΦEMI Y - 79 photomultiplier for the wavelength range from 400nm - 700nm. Photomultiplier voltage is set to 2300V.

Emission spectra study was carried out for each group and the results were multiplied by the correction factor which correspond to their respective wavelengths.

The spectral analysis of the first and second sets with their corresponding peak values are given in Fig.14. It is tacitly assumed that $I_{photo}$ is directly proportional to emission intensity.

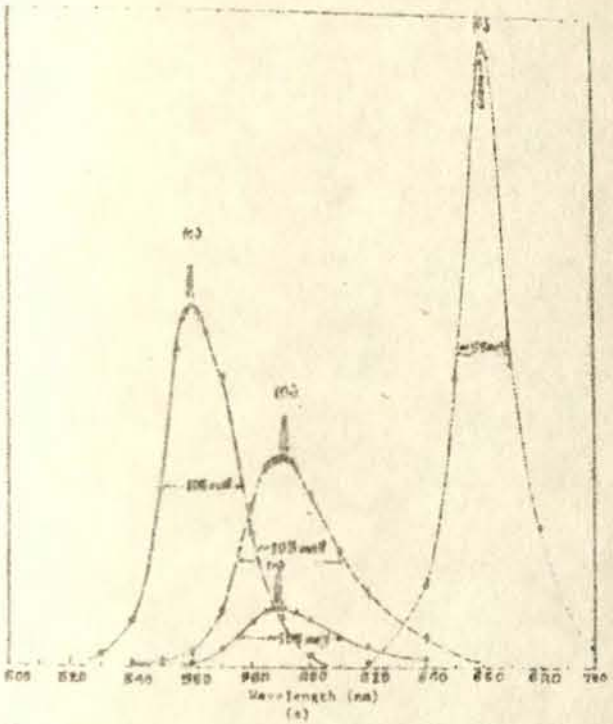

Fig.14: Emission spectra of the first (a) and second (b) sets of EL diodes under diode current of 20mA photomultiplier voltage of 2300V. Peak emission wavelength and half bandwidth energies are shown for each EL diode.

Fig.14 gives ample informations about the EL diodes. The peak height of the spectral curve gives the relative emission intensity in arbitrary units. Comparision of these relative emission intensities shows that red EL diodes are the most intense. Its intensity is almost double that of green I which is the 2nd most intense. As compared to yellow I, the intensity of these EL diodes is about ten times higher.

The bandwidth of the spectral curve gives some clue about the nature of impurities. Half bandwidths are evaluated to quantify the comparisons. Broad spectrum characterizes impurity levels which are responsible for transitions corresponding to different energy levels. For impurity levels extending to bands, transitions corresponding to different photon energies are possible and this broadens the spectrum. If there is only one impurity level, sharp peak is observed. In line with this argument, red EL diodes show relatively narrower band widths as compared to the rest. This implies that there are more definite energy states at which recombinations take place in these EL diodes. Close observation of EL diodes of the 2nd set shows small secondary peaks to the right (for green) and to the left (for yellow) from the primary peaks. The presence of these secondary peaks reveals the presence of different recombination levels apart from the primary ones and they are associated with different impurity levels which correspond to different energies. These additional secondary peaks correspond to energies of orange and yellow bands in yellow and green EL diodes, respectively.

Usually, the main and secondary peaks are close to each other and it is difficult to resolve the two at higher temperature. Better resolution of the two could be possible at lower temperatures (i.e at a temperature of liquid nitrogen, 77K, or liquid helium, 4K). At low temperatures, thermal (lattice) effects are suppressed and only effects of impurities are evident. Low temperature is characterized by freeze out of carriers.

When the peaks nearly overlap and cannot be resolved, the spectral shape could be unsymmetric as in $G_{a_1}$ (Fig. 14a) or the two may be separated as in (Fig.15).

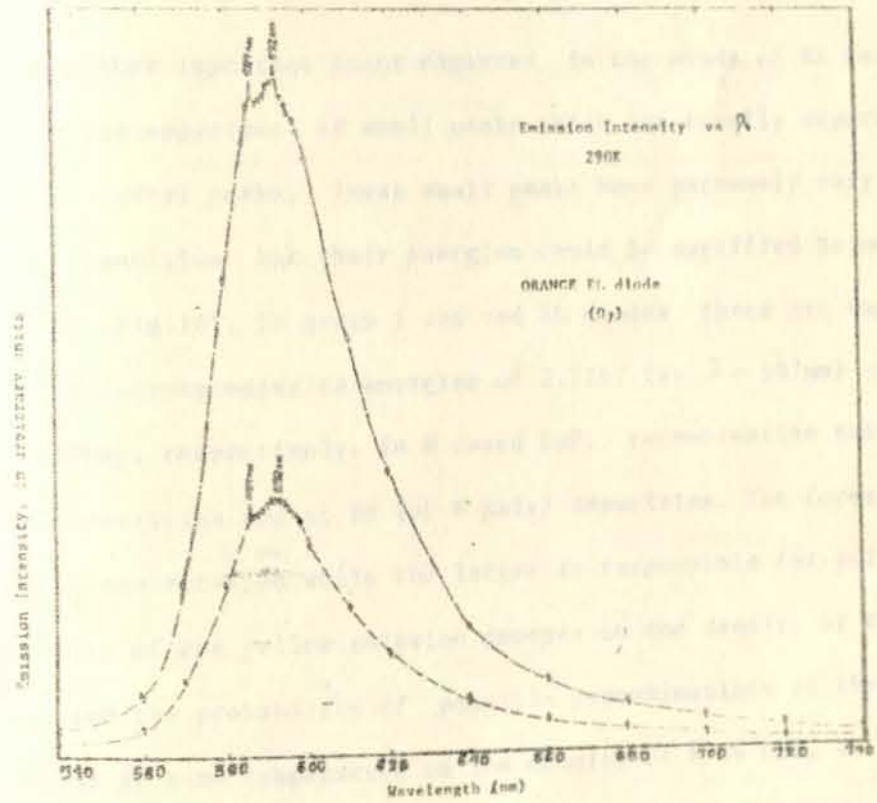


Fig.15: Emission intensity of orange EL diodes at 10 and 20mA diode currents and 2800V photomultiplier voltage. Two peak emissions are observed, the main peak at 592nm and secondary peak at 587nm, the 2nd corresponds to the yellow band energy.

In the latter case, it is possible to resolve the two and tell the energy corresponding to the secondary emission. This in other words would also give a hint to specify the energy of the impurity level corresponding to this secondary peak emission.

There is an overlap of the two peaks as the diode current increases to 30mA. This may be due to the heating effect of the current. As the diode is heated, more and more impurities are ionized and in addition band gap decreases and this may cause the initiallly separate energy levels to overlap. Transitions to such overlapped states result in a spectrum which is not finaly resolved.

The other important point observed in the study of EL emission spectra is the appearance of small peaks which are totally separated from the main (primary) peaks. These small peaks have extremely very small emission intensities but their energies could be specified beyond doubt. As shown in (Fig.16), in green I and red EL diodes there are negligibly small peaks corresponding to energies of 2.11eV (or $\lambda \simeq 587$nm) and 1.70eV (or $\lambda \simeq 730$nm), respectively. In N doped GaP, recombination takes place both at N impurities and at NN (or N pair) impurities. The former is responsible for green emission while the latter is responsible for yellow emission. The intensity of the yellow emission depends on the density of the available NN states and the probability of possible recombinations at these NN states. These depend at room temperature on the density of N in GaP. If N is large in concentration, the transitions at NN pairs may dominate in this compound semiconductor[56]. The reduced intensity of yellow emission in green GaP therefore, indicates low concentration of N in GaP.

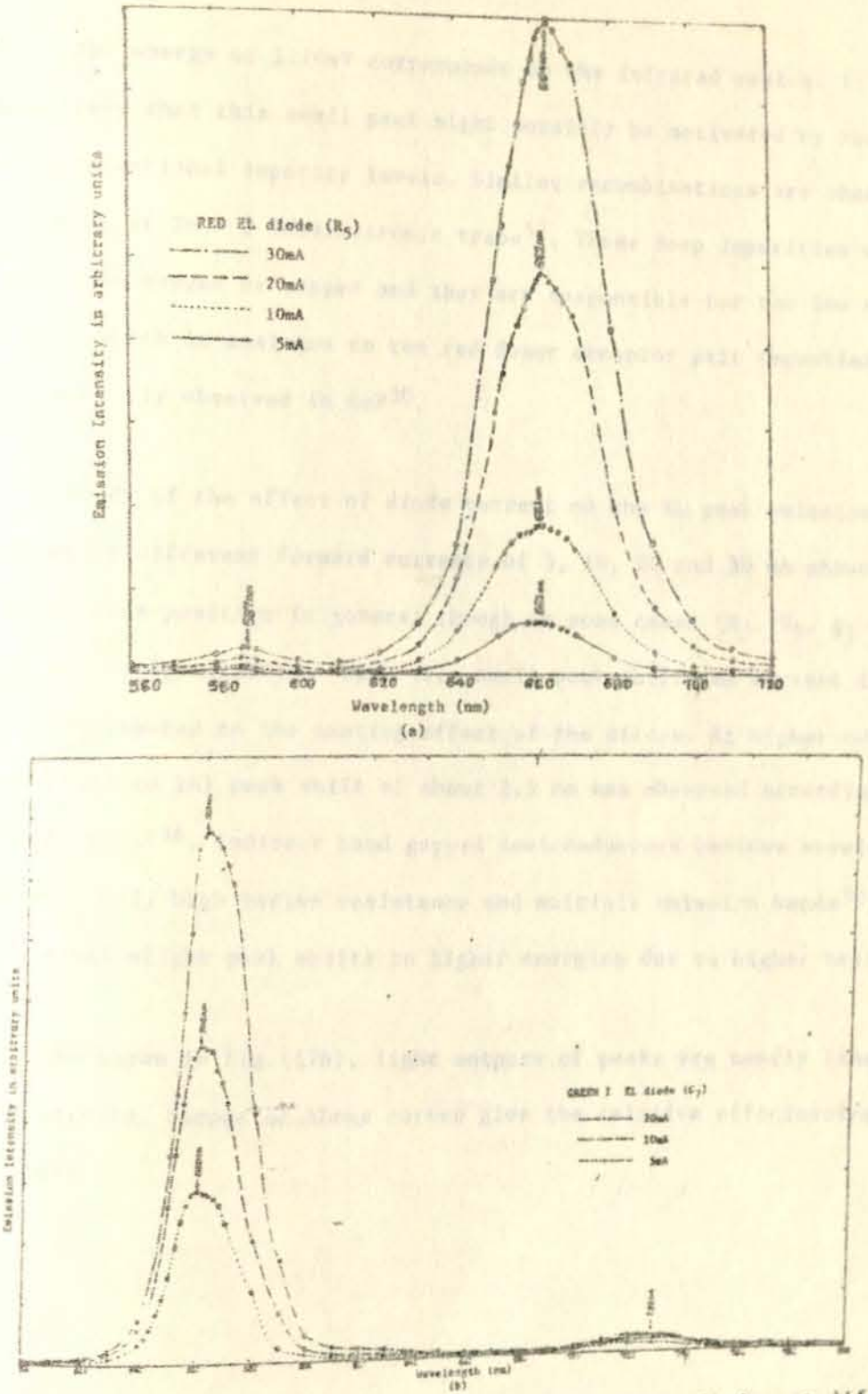


Fig.16: Emission spectra of red (a) and green I (b) EL diodes at different diode currents and 2300V photomultiplier voltage. In red EL diodes, small peaks are observed at 730nm and in green ones at 587nm. The positions of these peaks remained constant irrespective of the diode currents.

The energy of 1.70eV corresponds to the infrared region. It is more likely that this small peak might possibly be activated by relatively deep unintentional impurity levels. Similar recombinations are observed in red GaP EL at Zn - O isoelectronic traps[57]. These deep impurities may probably be oxygen or copper and they are responsible for the low energy emission which is analogus to the red donor acceptor pair recombination bands commonly observed in GaP[30].

Study of the effect of diode current on the EL peak emission position at different forward currents of 5, 10, 20 and 30 mA showed no shift in peak position in general though in some cases ($R_3$, $O_3$, $g_1$ of Fig.17) there were slight shifts. Such very small peak shifts as current increases may be attributed to the heating effect of the diodes. At higher currents (from 10 $\mu$A to 1A) peak shift of about 2.5 nm was observed according to Craford et al[36]. Indirect band gapped semiconductors besides showing low quantum yield, high series resistance and multiple emission bands[30], do also reveal slight peak shifts to higher energies due to higher heating.

As shown in Fig.(17b), light outputs of peaks are nearly linear with currents. Slopes of these curves give the relative efficiencies of the EL diodes.

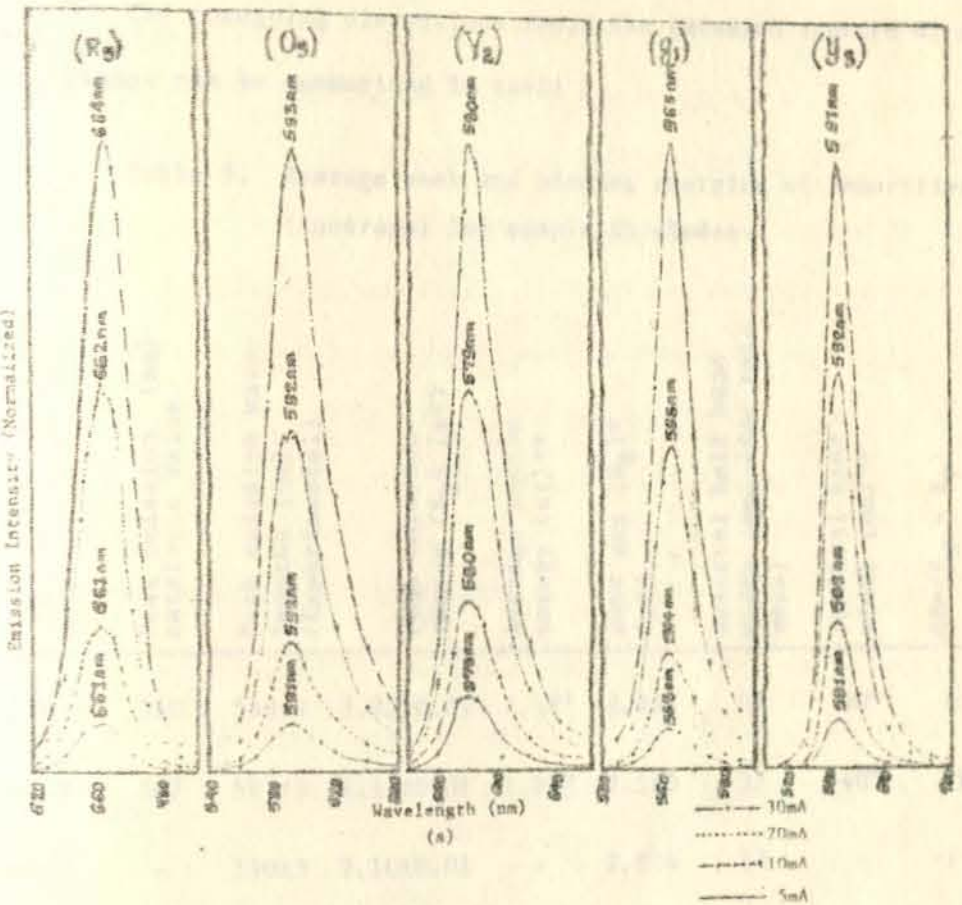


Fig.17: (a) Peak emissions of different colored EL diodes at 5,10,20 & 30 mA diode currents. The peak intensities corresponding to the 30mA are normalized. The differences in the intensities at smaller diode currents indicate the variations of peak intensity values with current as shown in (b) The differences in slopes observed in (b) reveal differences in efficiencies of the different EL diodes.

The foregoing discussions about the emission spectra of differ EL diodes can be summarized in table 5.

Table 5. Average peak and binding energies of impurities (isotraps) for sample EL diodes.

| LED color | Peak emission (nm) catalogue value | Peak emission wavelengths (nm) (Experimental) | Peak emission energy ($E_p$) (eV) | Average photon energy (eV)** | Band gap ($E_g$)* (eV) | Spectral half band width (nm) (for this work) | Spectral band width (nm)** | $\Delta E=(E_g - E_p)$ (meV) |
|---|---|---|---|---|---|---|---|---|
| GREEN I | 560 | 560±3 | 2.22±0.01 | 2.18+ | 2.261 | 27 | 30+ | 41 |
| YELLOW I | 587 | 587±3 | 2.11±0.01 | 1.97+ | 2.180 | 37 | 40+ | 70 |
| ORANGE | - | 590±3 | 2.10±0.01 | - | 2.086 | 37 | - | -14 |
| RED | 660 | 662±8 | 1.87±0.02 | 1.91 | 1.925 | 18 | 28 | 55 |
| GREEN II | - | 562±7 | 2.21±0.03 | 2.18+ | 2.261 | 23 | 30 | 51 |
| YELLOW II | - | 593±3 | 2.09±0.01 | 1.97+ | 2.180 | 40 | 40+ | 90 |

* Calculated on the assumption that the EL diodes are made from Ga $As_{1-x}$ $P_x$ ternary alloys.

** Taken from Bergh and Dean, 1976, page 33, table 1.3, for comparison purposes.

\+ The N doped Ga P results are considered.

$\Delta E$ is the difference between the energy gap ($E_g$) and the peak emission energy ($E_p$).

The binding energy of Zn in Ga (As, P) EL diodes is within $\sim 30 - \sim 65$ meV[26,36] and that of Te is about 90 meV[26]. Hence, in yellow EL diodes where $(E_D + E_A) = 90$ meV, recombination might be through Te donors. In others, it might be through zinc acceptors or by pair emission (donor to acceptor). Transitions can also take place from isoelectronic traps to acceptors or from donors to hole traps. In the latter three cases $\Delta E$ is the sum of two binding energies and it is difficult to tell the nature and the type of the impurity.

## 3.5 Thermal Band Gap Determination

Practically all of the EL diodes have negligibly small reverse currents because of their large energy gaps. To determine band gap under forward current the following approach was adopted from Sze[18]

$$I_o \sim [T^3 \exp(-E_g/K\,T)]T^{\gamma/2}$$

$$\sim T^{3+\gamma/2} \exp(-E_g/KT) \qquad (20)$$

$I = I_o\,[\exp(qV/nKT)-1] \sim A \exp[-(E_g - qV/n)/KT]$ where A is a constant.

$$\ell n\, I = -(1/T)\,[E_g + (qV/n)]/K \qquad (21a)$$

Plotting $\ell n\, I$ versus 1/T yields: $E_g$ as

$$E_g = qV/n - K[\ell nI/(1/T)] = qV/n - K\,(\text{slope}) \qquad (21b)$$

The plot of $\ell n\, I$ vs (1/T) is shown in Fig. 18 with average $E_g$ values in table 6.

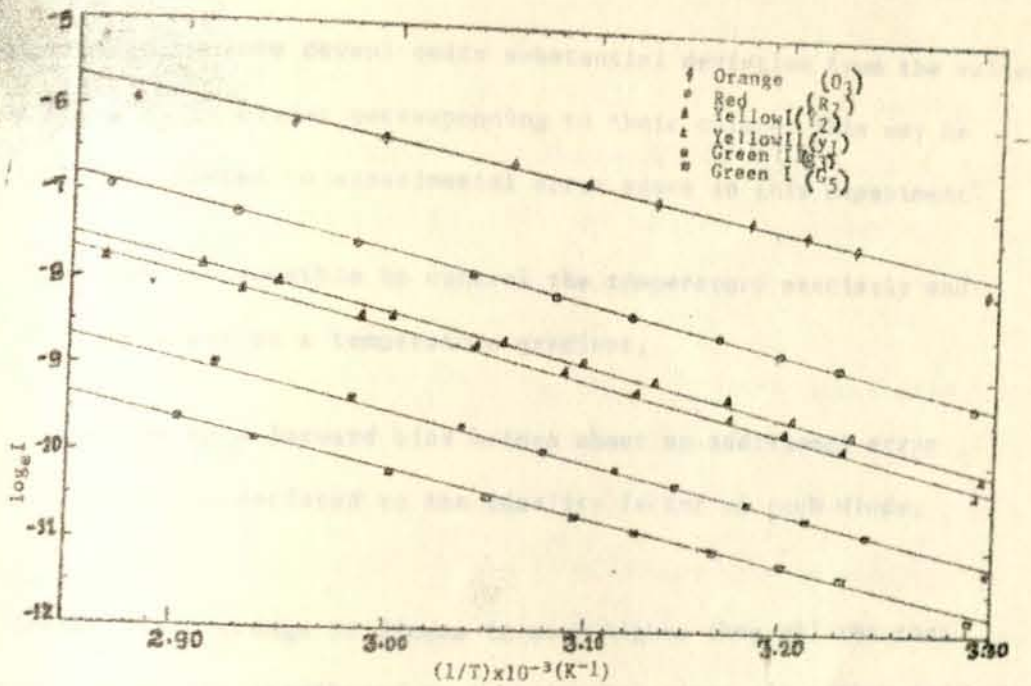


Fig.18: Natural logarithm of diode current plotted against the reciprocal of temperature for representative sample EL diodes. The straight lines indicate best fits to the experimental data points.

Table 6. Experimentally determined thermal energy gap values

| LED color | $E_g$(eV) exptal. | $E_g$(eV) theoretical ($Ga As_{1-x}P_x$ EL diode) |
|---|---|---|
| GREEN I | 2.21 ± 0.17 | 2.261 |
| YELLOW I | 2.07 ± 0.04 | 2.180 |
| ORANGE | 2.52 ± 0.06 | 2.086 |
| RED | 1.76 ± 0.12 | 1.925 |
| GREEN II | 1.82 ± 0.06 | 2.261 |
| YELLOW II | 1.86 ± 0.06 | 2.180 |

Band gap measurements reveal quite substantial deviation from the values of Ga $As_{1-x}$ $P_x$ EL diodes corresponding to their colors. This may be partially attributed to experimental error since in this experiment,

i) it was not possible to control the temperature precisely and there might be a temperature gradient,

ii) the use of a forward bias brings about an additional error which is associated to the ideality factor of each diode.

The deviation of orange EL diodes is much higher than all the rest. This is not at all attributed to experimental error. It rather indicates that the diodes might have possibly been made from some other compounds or ternary alloys.

## IV CONCLUSIONS

The aim of this work was to study injection EL in p-n junctions. A set of 34 samples divided into two different groups depending on their origin were studied optically and electrically. Among the most important of the parametric studies I-V, C-V and emission intensity were chosen and the following conclusions have been drown.

1. From I-V data, the ideality factor obtained ranges from 1 to 2, indicating some deviation from the ideal Schottky diode equations in which the ideality factor assumes the value of 1 under forward bias. This implies that the diodes are of wide band gap semiconductors. The reverse current which is less than $10^{-12}$A (between 0 - 3 volts) also gives an additional confirmation of the wide band gap nature.

2. Results from band gap and peak emission energy measurements and comparison with the experimental works carried out on similar EL diodes show that the sample LEDs are of Ga (As, P). The condition of orange EL diode however, needs further investigation.

3. C-V results indicate abrupt junctions for all the diodes with built-in potentials between 1.6 - 2.9V. This again supports the wide band gap nature (i.e. $V_{bi} \sim E_g$). In addition, the substrate dopant concentration ($N_B$) is about $10^{16}$ to $10^{17}/cm^3$ under the assumption that the junction area of the diode is about $10^{-3}cm^2$. Thus, all the EL diodes are nondegenerate at least on one side.

4. Emission intensity which is proportional to the photomultiplier current has an exponential dependence on diode voltage. This exponential dependence strictly holds within the voltage range over which the ideality factor remains constant.

5. Comparison of emission intensities of the different colors and types of EL diodes show that the Red(R) ones are the most intense followed by Green I(G). The couses are direct radiative transitions in the former and band enhancement by N isoelectronic traps in the latter.

6. Secondary peak emissions observed in Orange(O), Red(R) and Green I (G) EL diodes are due to slightly separated impurity levels, unintential deep trap levels and recombinationsat NN pair traps, respectively.

7. Only slight peak shift was observed as a result of the diode current. This can be attributed to junction current heating effect, but further measurement with more sensitive instruments will be required to find the appropriate relation between the two.

8. Measurement of the binding energy ( $\Delta E$) of the dopants in each EL diode has shown a result in the range from 40meV (for Green I) to 90meV (for yellow II). This result is in good agreement with the data published earlier for Ga P:N. No similar comparison could be made for Orange & Red due to lack of data.

REFERENCES

1. G.J. Deboo and C.N. Burrous, Integrated Circuits and Semiconductor devices: Theory and Application, McGraw-Hill, Singapore (1977), page 286.

2. A.A. Bergh and P.J. Dean, Light Emitting diodes, Oxford (1976), page 228.

3. A.A. Bergh, Reference 2, page 526.

4. A.A. Bergh, Reference 2, page 528.

5. A.K. Chin et al, Jap.J. Appl.Phy. PI.21(9), 1308, (1982).

6 P.J. Dean, III-V Compound Semiconductors, Ed. by J.I. Pankove, Springer-Verlag, Berlin (1977), page 64.

7. A.A. Bergh, Reference 2, page 3.

8. P.J. Dean, Reference 6, page 65.

9. A.A. Bergh, Reference 2, page 36.

10. P.J. Dean, Reference 6, page 68.

11. A.A. Bergh, Reference 2, page 394.

12. A.A. Bergh, Reference 2, page 35.

13. J.I. Pankove, Reference 6, page 11.

14. A.A. Bergh, Reference 2, page 55

15. P.J. Dean, Junction Electroluminescence, Ed. by R. Wolfe, Academic Press, New York (1969), page 47.

16. P.J. Dean, Reference 15, page 19.

17. P.J. Dean, Reference 15, page 21.

18. S.M. Sze, Physics of Semiconductor Devices, John Wiley, USA (1981), page 87.

19. S.M. Sze, Reference 18, page 90.

20. S.M. Sze, Reference 18, page 92.

21. S.M. Sze, Reference 18, page 76.

22. H. Kressel et al., J. Appl. Phy. 41(11), 4692, (1970).

23. P. Mischel and G. Schul, (1970) Symp. on Ga As, paper 21, page 188.

24. H. Kressel et al, J. Appl. Phy. 40(5), 2248, (1969).

25. Onton and Lorenz, (1970) Symp. on Ga As, paper 26, page 222.

26. Onton and Lorenz, J. Appl. Phy. 42(9), 3420, (1971).

27. A.A. Bergh, Reference 2, page 384.

28. S.M. Sze, Reference 18, page 691.

29. P.J. Dean, Reference 6, page 78.

For example 30. A.H. Herzog et al.,J. Appl. Phy. 40(4), 1830 (1969).

31. Holenyak et al.,(give $x_c = 0.46$), J. Appl. Phy. 43(10), 4148 (1972).

32. M.H. Lee et al., J. Appl. Phy. 46(3), 1290 (1975).

33. Nelson et al., J. Appl. Phy. 47(8), 3625 (1976).

34. Campbell et al. J. Appl. Phy. 45(10), 4543 (1974).

35. Grovset al., Appl. Phy. lett 19, 184 (1971).

36. Craford et al., J. Appl. Phy. 43(10), 4075 (1972).

37. P.J. Dean, Reference 6, page 77.

38. P.J. Dean, Reference 15, page 12.

39. R.Z. Bachrach and O.G. Lorimor, J. Appl. Phy. 43(2), 500 (1972).

40. A.A. Bergh, Reference 2, page 291.

41. Dierschke and Pearson, J. Appl. Phy. 41(1), 321 (1970).

42. Luther et al., J. Appl. Phy. 44(9), 4072 (1973).

43. Ladany and Wang, J. Appl. Phy. 43(1), 237 (1972).

44. P.J. Dean, Reference 18, page 80.

45. Daniel A Grenauney and Herzog, J. Appl. Phy. 39(6), 2783 (1968).

46. Z. Zaeschmar and R.S. Speer, J. Appl. Phy. 50(9), 5686 (1979).

47. H. Schade et al., J. Appl. Phy. 42(12), 5072 (1971).

48. L. Levi, Applied Optics Vol.1, John Wiley, USA (1968), page 250.

49. H. Schade et al., J. Appl. Phy. 44(9), 3783 (1970).

50. Shih et al., J. Appl. Phy. 39(3), 1557 (1968).

51. J.M. Ralston, J. Appl. Phy. 44(6), 2635 (1973),

52. S.M. Sze, Reference 18, page 848.

53. A.A. Bergh, Reference 2, page 57.

54. C. Lawther et al., Jap. J. Appl. Phy. 19(5), 939 (1980).

55. Handbook of Chemistry and Physics CRC (1975-1976) 56th ed.
E-217 and E-230.

56. A.A. Bergh, Reference 2, page 197.

57. J.M. Dishman and D.F. Daly, J. Appl. Phy. 43(11), 4693 (1972).

DECLARATION

I hereby declare that this thesis which is entitled "Experimental Studies of Injection Electroluminescence in p-n Junctions" and submitted in partial fulfillment for the Master of Science Degree is my original work done under the supervision of Dr. P. Hrushka. Spurces of relevant informations including books and articles used in this work are duly acknowledged.

Gelana Amente

The thesis was submitted
to the Physics Department
Graduate Committee on
June 19, 1987

This thesis has been submitted for examination with my approval as University Advisor.

P. HRUSHKA